ASSESSMENT OF BURIED PIPELINES COATING AND THE CASE FOR A NEW REFLECTOMETRY BASED TECHNOLOGY

A Thesis

by

TRISTAN CHRISTOPHE LÉONCE PETIT DE SERVINS D'HÉRICOURT

Submitted to the Office of Graduate and Professional Studies of
Texas A&M University
in partial fulfillment of the requirements for the degree of

MASTER OF SCIENCE

Chair of Committee,	Homero Castaneda-Lopez
Committee Members,	Ramesh Talreja
	Tahir Cagin
Head of Department,	Ibrahim Karaman

December 2017

Major Subject: Materials Science and Engineering

ABSTRACT

Corrosion control of buried assets usually involves a redundant shield: a coating system as a physical barrier, and a cathodic protection system as an ad hoc defense. Characterization and localization of defects in the coatings of such assets is critical, since large defects, if left unrepaired, will not only leave the asset locally prone to corrosion, but also drain and weaken the cathodic protection for the entire structure.

Electrochemical impedance spectroscopy has been used in order to study the influence of different types of defects on the insulating capabilities of coal tar coating. Experimentation and research has led the author of this thesis to design a reflectometry based method to provide both localization and characterization of such defects. In the energy industry, most pipelines consist of several parallel lines and this method makes the most of this feature in order to overcome difficulties usually associated with time domain reflectometry, specifically the quest for reliable and adaptable baselines.

The method has been tested with success in both laboratory and field conditions. The conclusion of these tests acknowledges limitations in terms of operational distance for practical applications of this technique and confirms its usefulness for the detection of coating defects as well as other features for multiple pipelines.

ACKNOWLEDGMENTS

The crews from ConEd have always been helpful and resourceful during the testings at countless manholes in Queens, the Bronx and Manhattan and I thank them for welcoming me among them like they did.

I am very grateful towards my advisor and friend Dr Homero Castaneda, and his wife Dr Ayako Yajima for the precious guidance and support they kindly provided throughout my studies.

The National Corrosion and Materials Reliability Center was a very nice place to work at, and I will keep very good memories of the research environment I enjoyed there with my lab mates.

CONTRIBUTORS AND FUNDING SOURCES

Contributors

This work was supervised by a thesis dissertation committee consisting of Professor Homero Castaneda-Lopez and Professor Tahir Cagin of the Department of Materials Science and Engineering and Professor Ramesh Talreja of the Department of Aerospace Engineering. Graduate study, as well as the project that inspired a large part of this thesis was funded by the Consolidated Edison Company of New-York

All work for the thesis was completed independently by the student.

Funding Sources

Graduate study, as well as the project that inspired a large part of this thesis was funded by the Consolidated Edison Company of New-York

TABLE OF CONTENTS

Page

LIST OF FIGURES

Page

LIST OF TABLES

Page

CHAPTER I

INTRODUCTION

Introduction to cathodic protection theory

Corrosion is a thermodynamic process driven by local potential discrepancies within a structure. Those differences of potential found across what are called cathodic and anodic sites, which are the specific locations for twin interfacial reactions: oxidation at the anodic site and reduction at the cathodic site. Oxidation is the dissolution reaction, which is harmful for metallic structures as it results in metal loss:

$$M \rightarrow M^{n+} + n\, e^{-}$$

For reduction, different reactions can occur, depending on many different parameters, most importantly the presence or absence of oxygen and the pH level. In neutral or alkaline conditions:

Oxygen reduction $2\, H_2O + O_2 + 4\, e^{-} \rightarrow 4\, OH^{-}$

or

Water electrolysis $2\, H_2O + 2\, e^{-} \rightarrow H_2 + 2\, OH^{-}$

In acid conditions:

Oxygen reduction $4\, H^{+} + O_2 + 4\, e^{-} \rightarrow 2\, H_2O$

or

Hydronium reduction $2\, H^{+} + 2\, e^{-} \rightarrow H_2$

The core concept of cathodic protection is therefore to inhibit this oxidation reduction. Such a goal is achieved by shifting the potential of the structure to protect, and provide current to its cathodic sites. Two different diagrams are useful to understand two different aspects of this protection, the Pourbaix diagram and the Evans diagram.

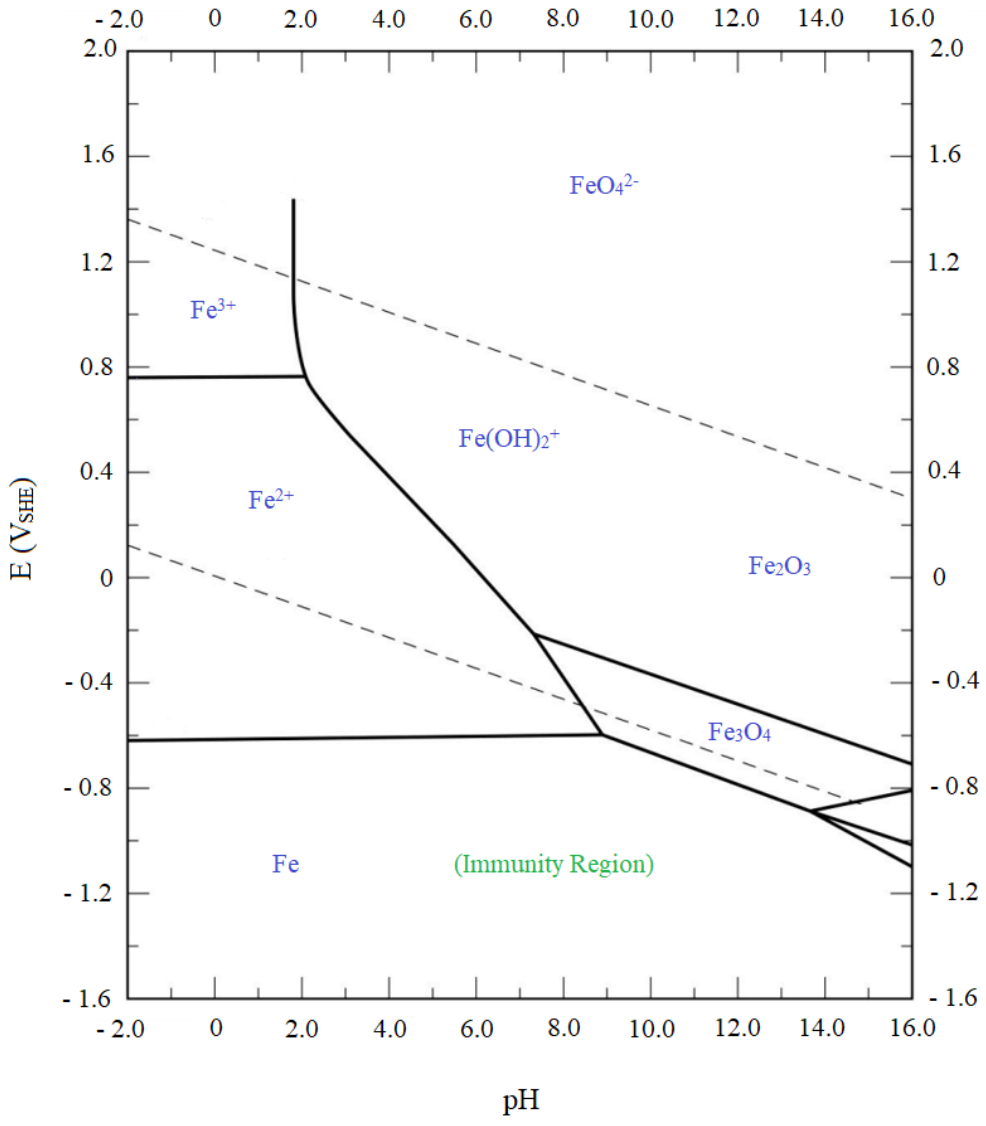

Figure 1: Pourbaix diagram of iron

The Pourbaix diagram plots the regions of thermodynamic stability for different phases of an electrochemical system. On figure 1, the Pourbaix diagram of iron, it can be seen that the lower part of the diagram is the region of stability of solid iron, which is called the immunity region since no iron ion is thermodynamically stable under those conditions. Cathodic protection aims to lower the potential of the entire structure to a potential belonging to the immunity region.

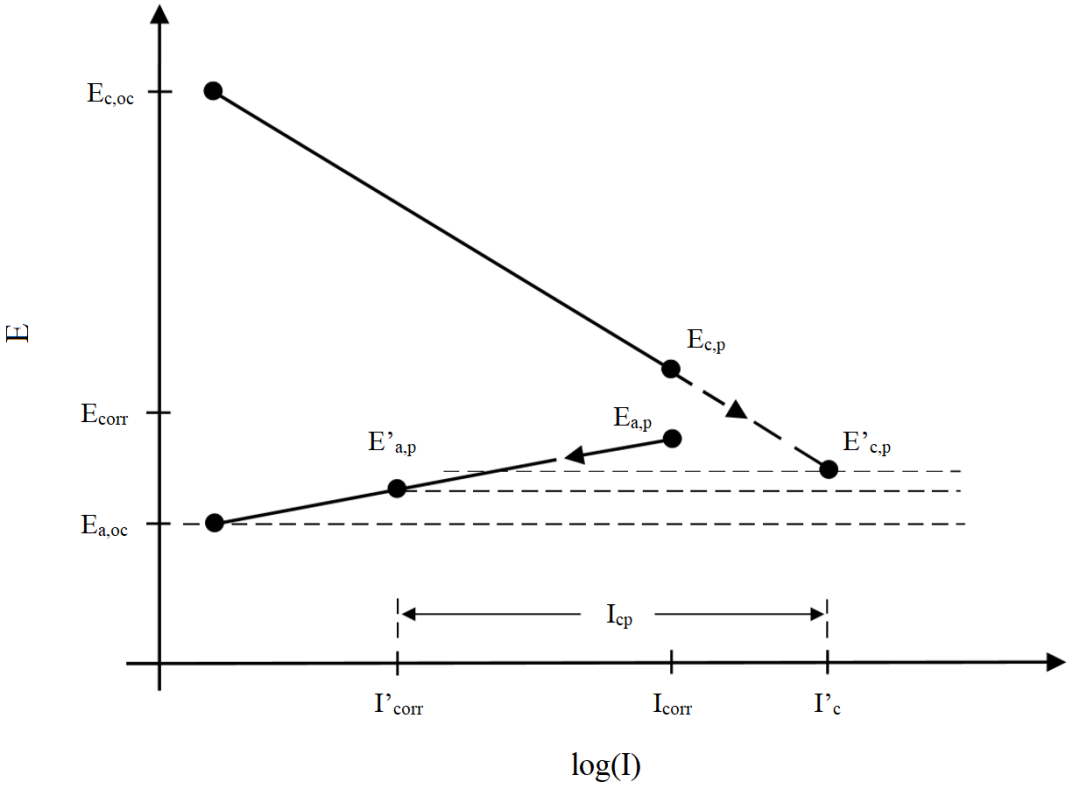

Figure 2: Evans diagram of a corrosion cell under cathodic protection

$E_{c,oc}$ Open circuit potential of the cathodic site

$E_{a,oc}$ Open circuit potential of the anodic site

$E_{c,p}$	Polarized potential of the cathodic site
$E_{a,p}$	Polarized potential of the anodic site
$E'_{c,p}$	Polarized potential of the cathodic site with cathodic protection
$E'_{a,p}$	Polarized potential of the anodic site with cathodic protection
E_{corr}	Corrosion potential
I_{corr}	Corrosion current density
I'_{corr}	Corrosion (anodic) current density with cathodic protection
I'_{c}	Cathodic current density with cathodic protection
I_{cp}	Current density provided by the cathodic protection system

However, the sole consideration of potential does not explain the entire concept, as there is a finer understanding of the corrosion and protection mechanisms that comes with the consideration of current density at the interface between the metal and the electrolyte. The relationship between the potentials of the cathodic and anodic sites with the current density is proportional, based on the low or the high field, and as the current density increases those sites (and, by metonymy, those potentials) are said to become polarized. The specific reaction, the electrolyte chemistry, and the interface determine the polarization slopes of both the cathodic and the anodic sites, called the Tafel slopes. The action of the cathodic protection is to decouple the current densities at the cathodic and anodic sites, by providing a current that sets them apart. The corrosion current is not completely nullified, but reduced by several orders of magnitude, to a level leading to an acceptable corrosion rate.

Coatings of cathodically protected assets and importance of locating and repairing defects in such coatings

Cathodic protection can either be achieved with galvanic protection, comprising local sacrificial anodes connected to the structure, or with an impressed current system. For large structures, like pipelines, this latter option is preferred.

It is interesting to parallel, on the macroscopic scale of the cathodic protection system, the relationship potential shift and current density given by the Evans diagram with Ohm's law. Let us consider a theoretical metallic structure under cathodic protection, divided between two parts; an anodic site and a cathodic site.

β_a	Anodic Tafel coefficient
β_c	Cathodic Tafel coefficient
β	Average Tafel coefficient (weighted average of β_a and β_c)
ΔE	Corrosion potential shift
I_0	Current density unit
R	Resistance of the macroscopic system to remote earth
S	Surface of the interface between the metallic structure and the electrolyte

Potential shift definition	$\Delta E = E_{corr} - E'_{corr}$
Tafel's equation	$\Delta E = \beta \log\left(\frac{I_{cp}}{I_0}\right)$
Ohm's law	$\Delta E = R(I_{cp}S)$

The reason why buried assets under cathodic protection are coated lies within those simple equations; and it would be an overly simplistic thinking to believe that connecting a metallic structure to a power source delivering a voltage corresponding to the immunity zone of the Pourbaix diagram is enough to guarantee the safety of the structure.

Indeed, as it will be seen in a more detailed fashion in chapter VII, the order of magnitude of R, the resistance to remote earth of a naked buried metallic structure is inversely proportional to the square root of its surface. Therefore:

$$\Delta E \propto I_{cp}\sqrt{S} \qquad (1)$$

It is expected that it is cost effective to coat a buried asset in order to cut down the required current to protect it. What is less obvious, and what we have shown with the previous reasoning, is that it is impossible to reach the same corrosion rate as a structure with both cathodic protection and insulating coating with a structure using only cathodic protection. In order to maximize the protection efficiency, i.e. the cathodic protection current density, it is necessary to minimize the interface surface, and therefore to cover the structure with an impermeable coating. The cathodic protection will then serve as an ad hoc corrosion control system at the locations where the coating failed.

It ensues from the previous considerations that coating failures such as holidays will drain the cathodic protection of the entire structure, and therefore accelerate the corrosion of every other active anodic site of the structure.

Another reason that makes the detection and repair of coating failures in pipeline assets critical comes from a hard limit on the applied voltage. Indeed, the potential of a steel structure cannot be brought under -1200 mV versus CSE without having

unacceptable level of hydrogen production, which then leads to hydrogen embrittlement, dangerous increase of pH at the metal surface, and delamination of the coating. This imposes in turn hard limits on two dimensioning issues, namely how far apart can two cathodic protection rectifiers be, and how much damage the insulating coating can sustain, in order to maintain acceptable potential on the entire length of the pipeline to protect. Indeed, in some cases coating holidays can raise the potential of pipeline sections further from the rectifier above the protection criterion.

CHAPTER II

COATING DEFECTS CHARACTERIZATION AND TRANSMISSION LINE THEORY

Characterization of coating defects using Electrochemical Impedance Spectroscopy

The experimental first step of this research has been to simulate and study different defects in the coal tar coatings of pipeline samples. The dimensions of those samples are presented in Table 1.

Table 1: Dimensions of the pipeline samples used

Unit System	Length	Diameter	Thickness	Coating Thickness
Imperial	1 foot	3 inches	¼ inch	50 mils
Metric	30.48 cm	7.62 cm	6.4 mm	1.3 mm

Two types of defects have been simulated on these pipeline sample: holidays, which are a complete removal of the coating over a small surface, and delaminations, which are a disbondment of the coating.

Creating a holiday in a coated pipeline sample is a pretty straightforward process, and in this study power tools have been used to remove the coating without damaging the steel over a circular area. However, there is no standard, nor for that matter references in the literature for controlled delamination simulation. It was therefore required to come up with a creative design.

Different aluminium molds have been milled, the following procedure has been designed to build delamination simulators. First, the moulds are covered with several layers of adhesive paste, double-sided tape and plastic film to ensure good adherence to the mould throughout the process. Then fresh coal tar is then applied and spread evenly on top of the set (see Figures 3 and 4).

Figure 3: Aluminum molds, and prepared mold set

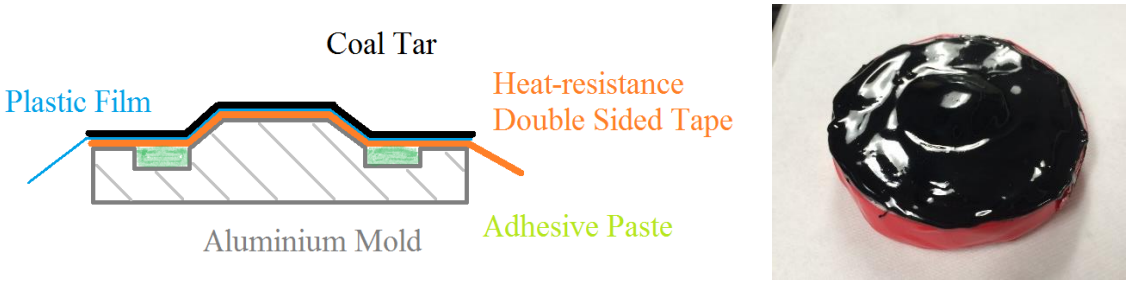

Figure 4: Cross section representation of a prepared mold set, and prepared mold set with fresh coal tar applied

The mold is then placed in an oven for curing. Once sufficiently cured (but not completely hardened), the plastic film is removed, and the coal tar sample is detached from the mould, and cut to size. This coal tar coating sample is then applied on a pipeline coating, where a holiday of the appropriate size has been previously made. The recoated pipeline is then put in the oven to undergo a second heat treatment (see Figures 5 and 6).

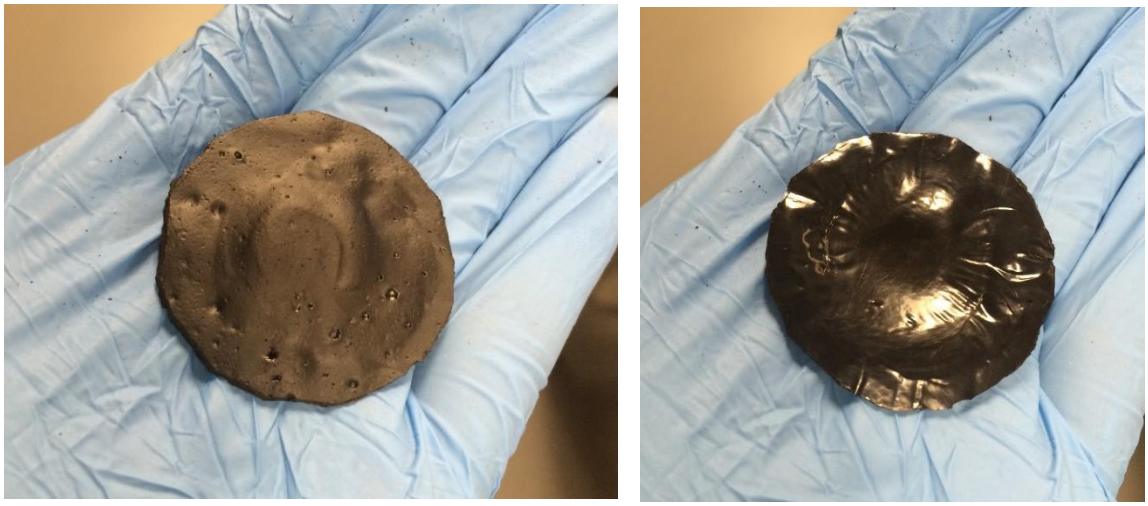

Figure 5: Outer and inner surfaces of the coal tar sample after partial curing

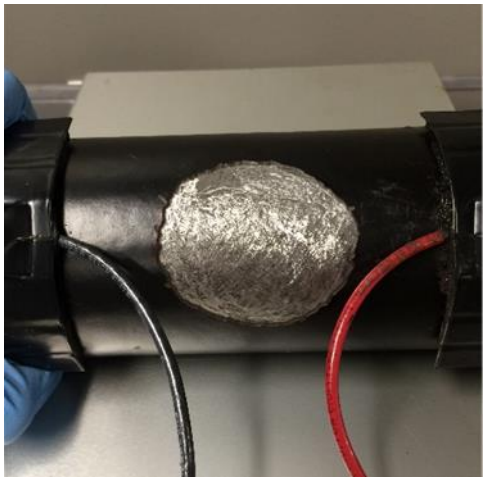

Figure 6: Initial holiday created in the pipeline coating, and simulated delamination after the recoating process

Seven different coating conditions have been simulated, and their characteristics are summarized in Table 2. The porosity is defined here as the total surface of mesoscopic pores. Those pores have been made with a 0.2 mm needle.

Table 2: Coating conditions simulated on seven pipeline samples

Coating Condition Name	Size of the Defect	Relative Porosity	Absolute Porosity
Intact Coating	none	0%	0 mm^2
Delamination S	0.5 $inch^2$ / 3.23 cm^2	0.04%	0.126 mm^2
Delamination M	1 $inch^2$ / 6.45 cm^2	0.02%	0.126 mm^2
Delamination L	2 $inch^2$ / 12.9 cm^2	0.04%	0.50 mm^2
Delamination L*	2 $inch^2$ / 12.9 cm^2	0.23%	3 mm^2
Holiday M	1 $inch^2$ / 6.45 cm^2	100%	1 $inch^2$ / 6.45 cm^2
Holiday L	2 $inch^2$ / 12.9 cm^2	100%	2 $inch^2$ / 12.9 cm^2

Copper cables have been welded at both ends of the pipeline samples. Plastic coering patches, plexiglass disks and silicone additions have been applied to insure the insulation of the whole sample. The pipeline samples have then been integrated to a larger laboratory set up, with large tanks filled with NS4, a solution designed to approximate the electrical behaviour and corrosion conditions of soil, as illustrated in Figure 7. The composition of NS4 is detailed in Table 3.

Table 3: Chemical composition of NS4

NS4 Solution	**KCl**	**$NaHCO_3$**	**$CaCl_2$**	**$MgSO_4$**
Concentration (g/L)	0.122	0.483	0.093	0.131

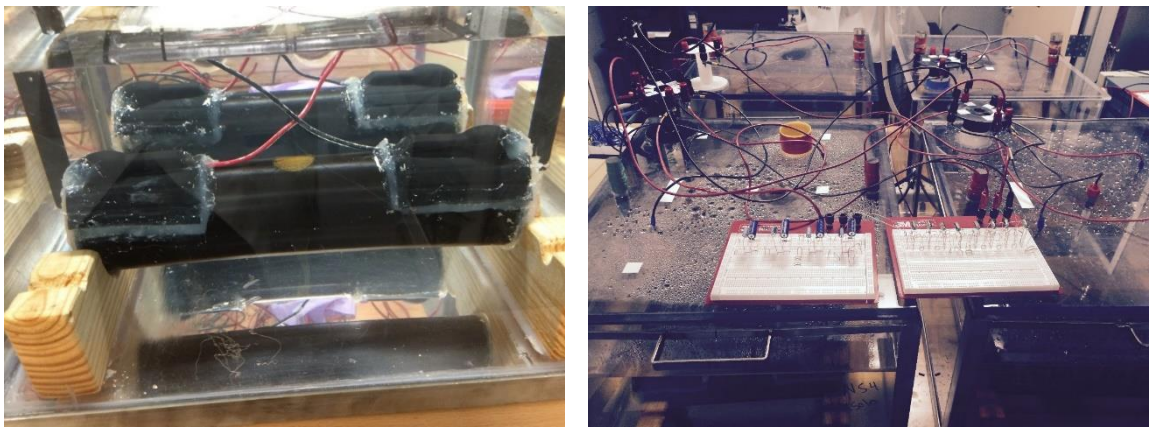

Figure 7: Laboratory setup illustrations

Electrochemical impedance spectroscopy testings have been performed with a Gamry 600+ potentiostat. Graphite rods have been used as counter electrodes. Figures 8, 9 and 10 show the Nyquist, complex and real impedance representations following the EIS characterization.

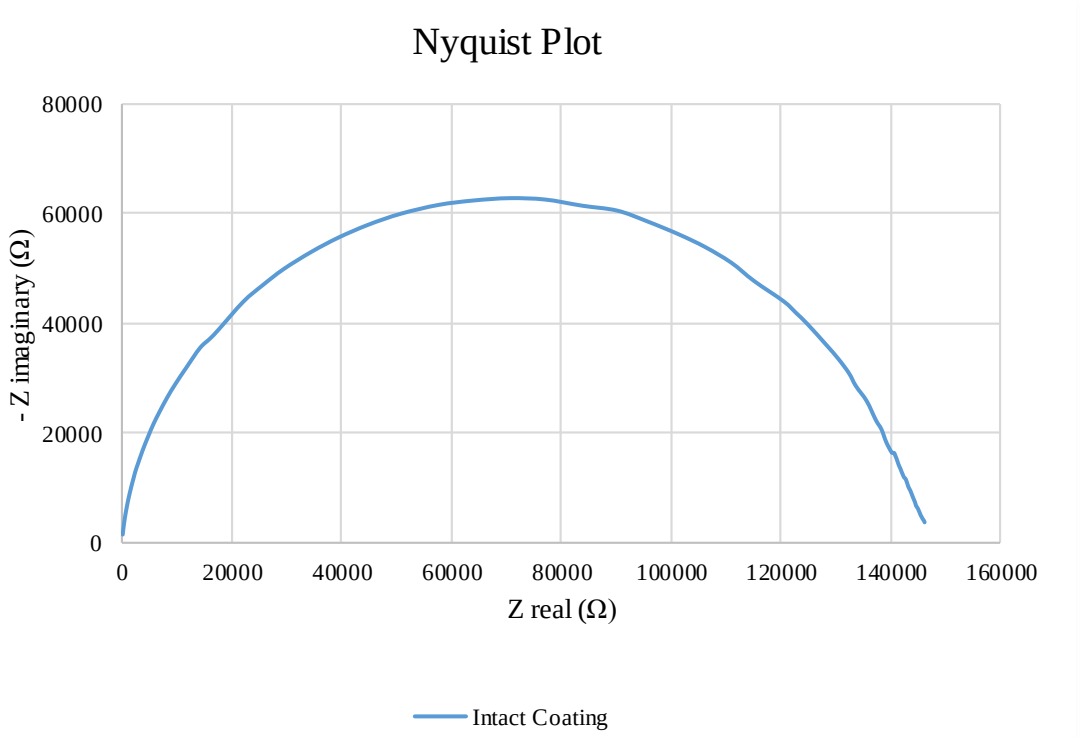

Figure 8: Nyquist plot of the pipeline sample with intact coating

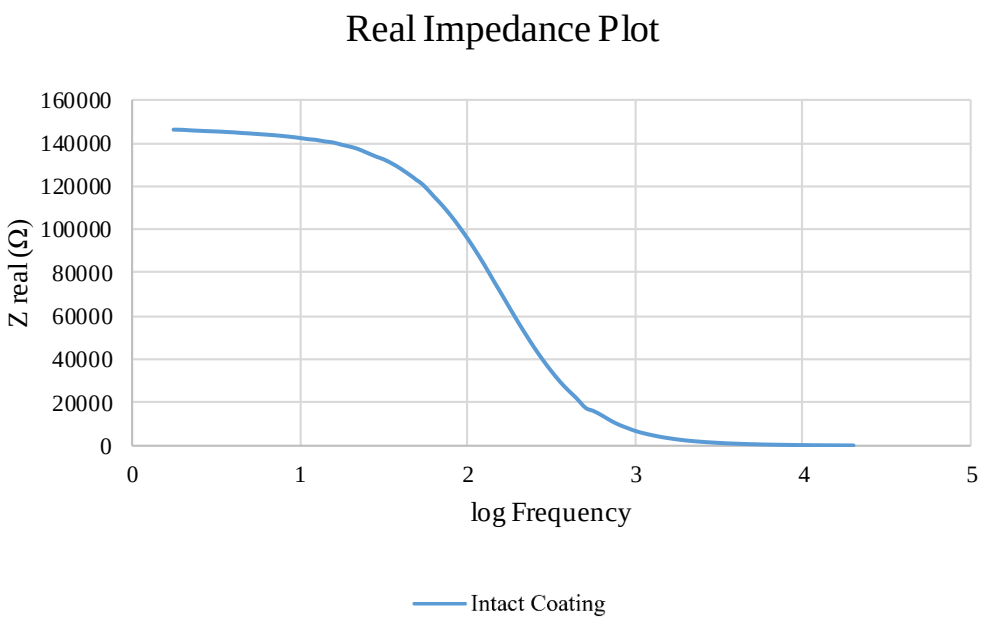

Figure 9: Real impedance plot of the pipeline sample with intact coating

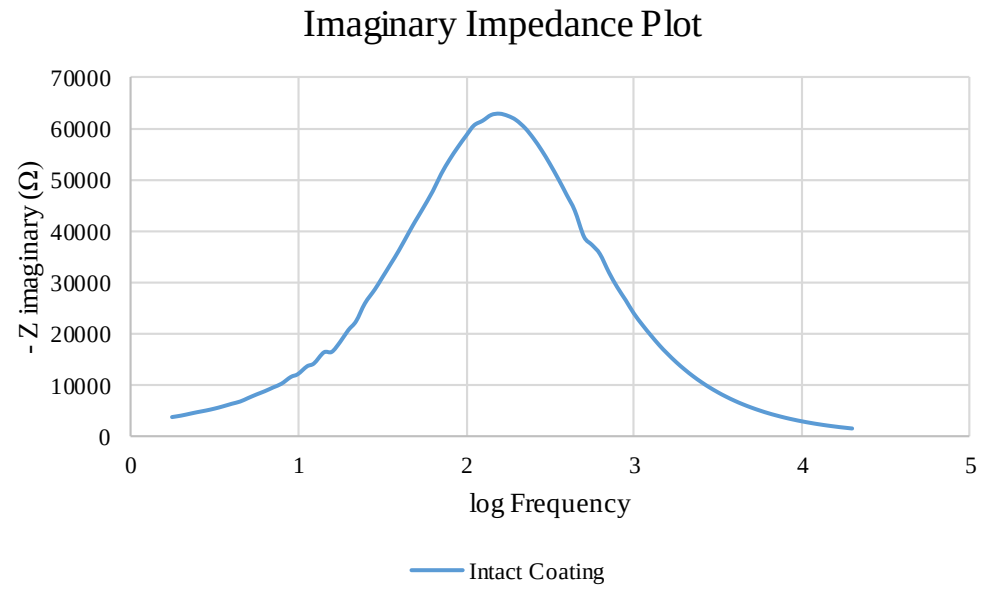

Figure 10: Imaginary impedance plot of the pipeline sample with intact coating

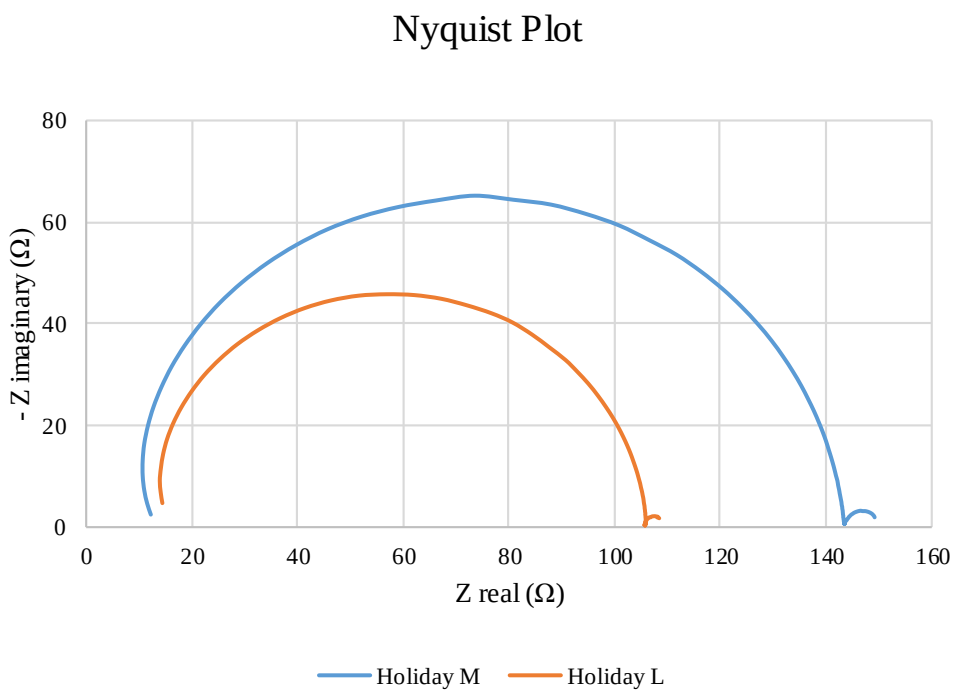

Figure 11: Nyquist plot of the pipeline samples with holidays

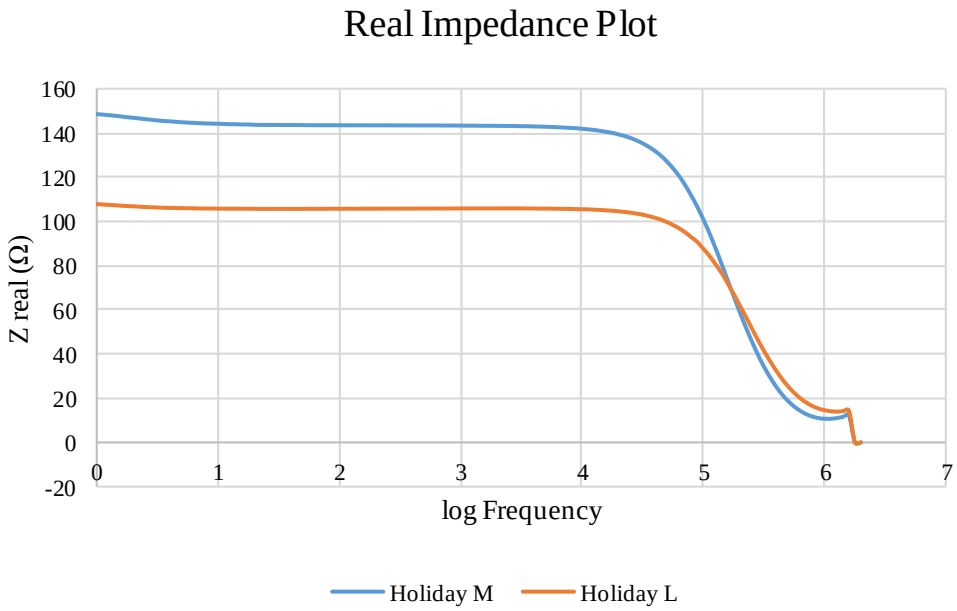

Figure 12: Real impedance plot of the pipeline samples with holidays

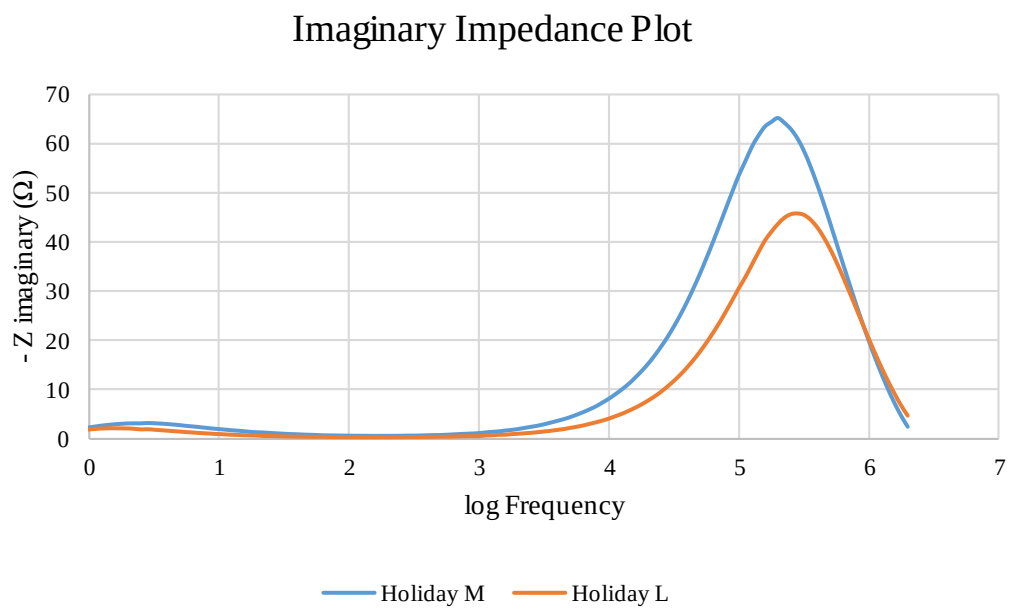

Figure 13: Imaginary impedance plot of the pipeline samples with holidays

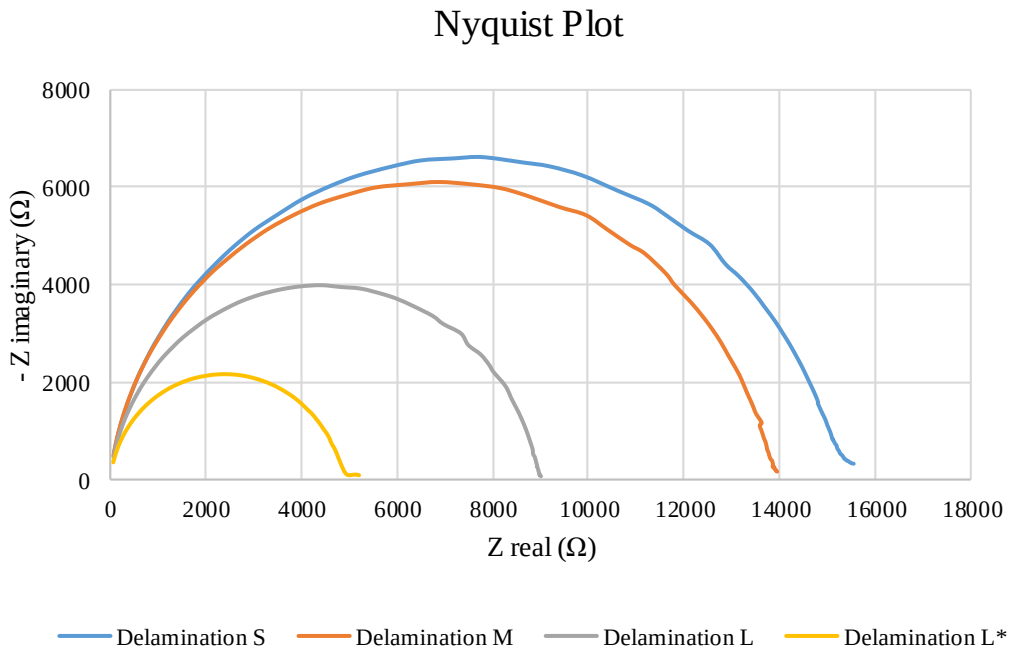

Figure 14: Nyquist plot of the pipeline samples with coating delaminations

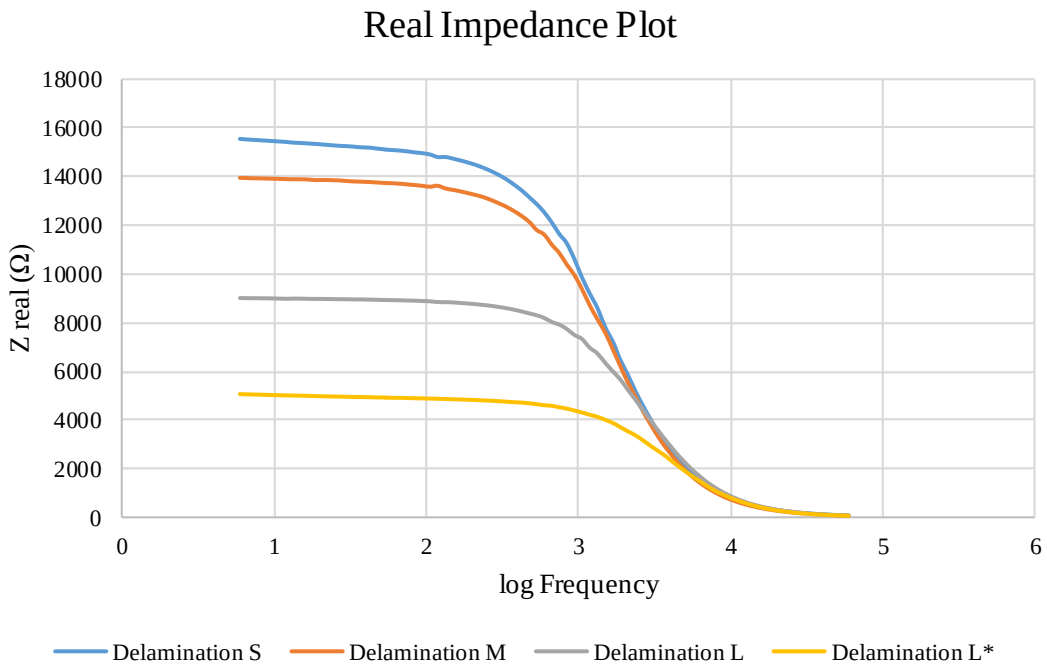

Figure 15: Real impedance plot of the pipeline samples with coating delaminations

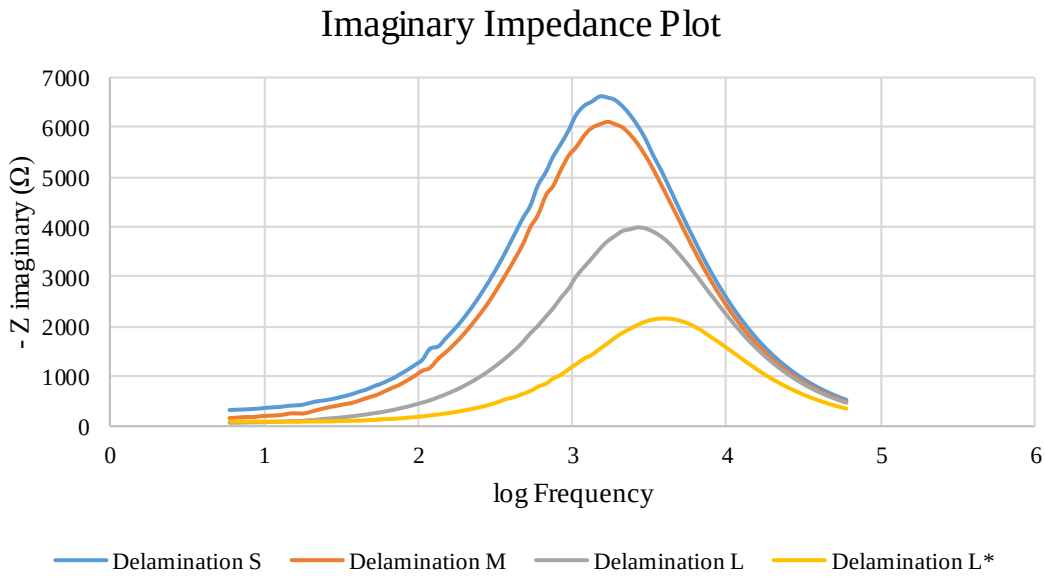

Figure 16: Imaginary impedance plot of the pipeline samples with coating delaminations

Figure 11, 12 and 13 show the EIS characterization for holiday and non holiday conditions in three different representations, respectively Nyquist, complex and real impedance plots. Figure 14, 15 and 16 show those same representations for simulated delaminations are in the substrate coating system. It is interesting to note that the measured impedance ratio between the two holiday samples is close to $\sqrt{2}$, which is coherent with the ratio of their surfaces, which is 2, and the theory of coating defect size previously described in chapter I. The small discrepancy can be explained by the slightly older age of the holiday M sample, which has been prepared and immersed in the NS4 tank a week earlier than the holiday L sample, and which therefore had a thicker passive layer.

The possibility of using impedance spectroscopy for a macroscopic structure coating assessment technology has been investigated, and this experimental set up has been integrated into an hybrid physical/electrical modelisation of a 40 km long pipeline as represented in the following electrical boards in Figure 17.

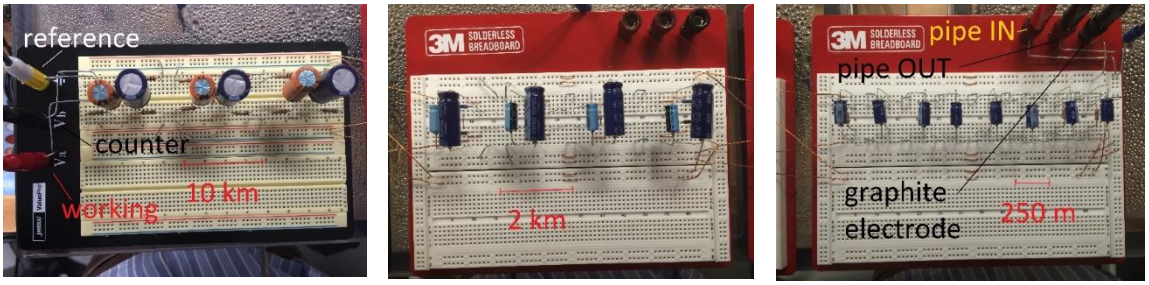

Figure 17: Breadboards of the hybrid modelisation

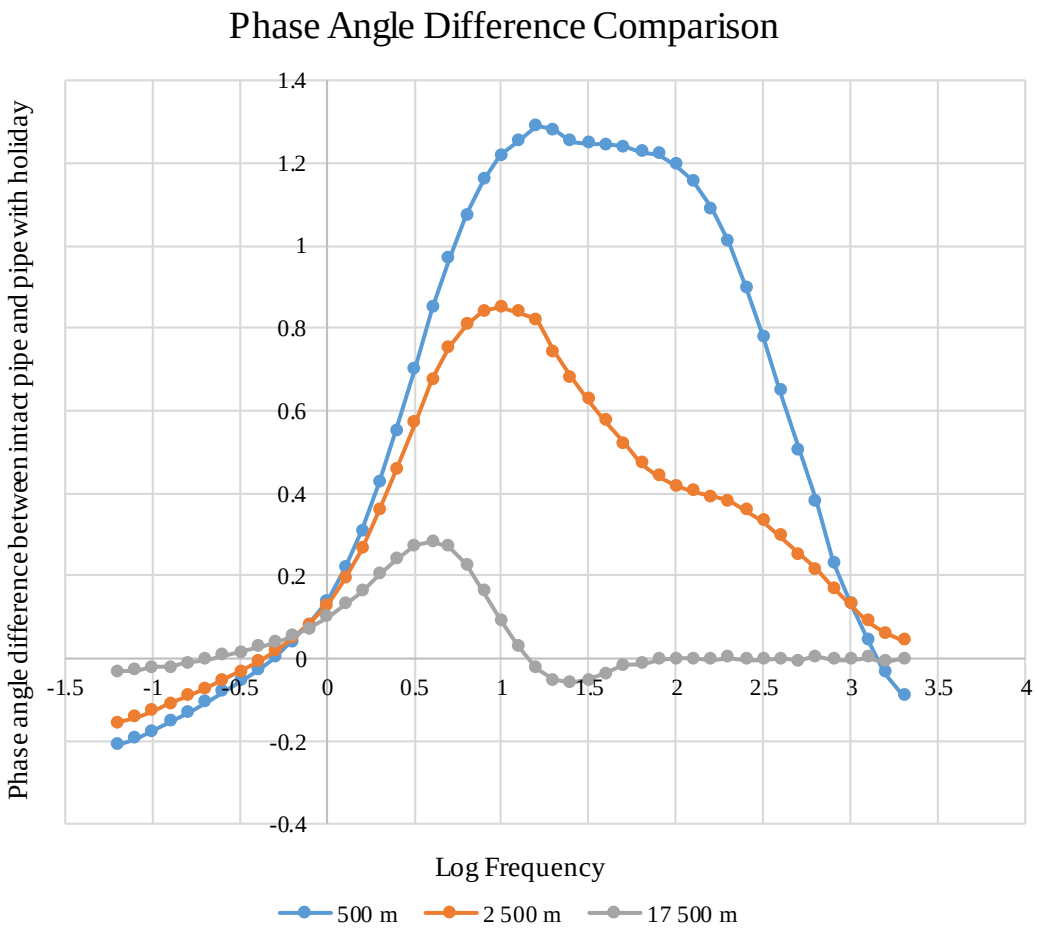

Figure 18: Phase angle comparison for a holiday defect placed at different distances in the hybrid model

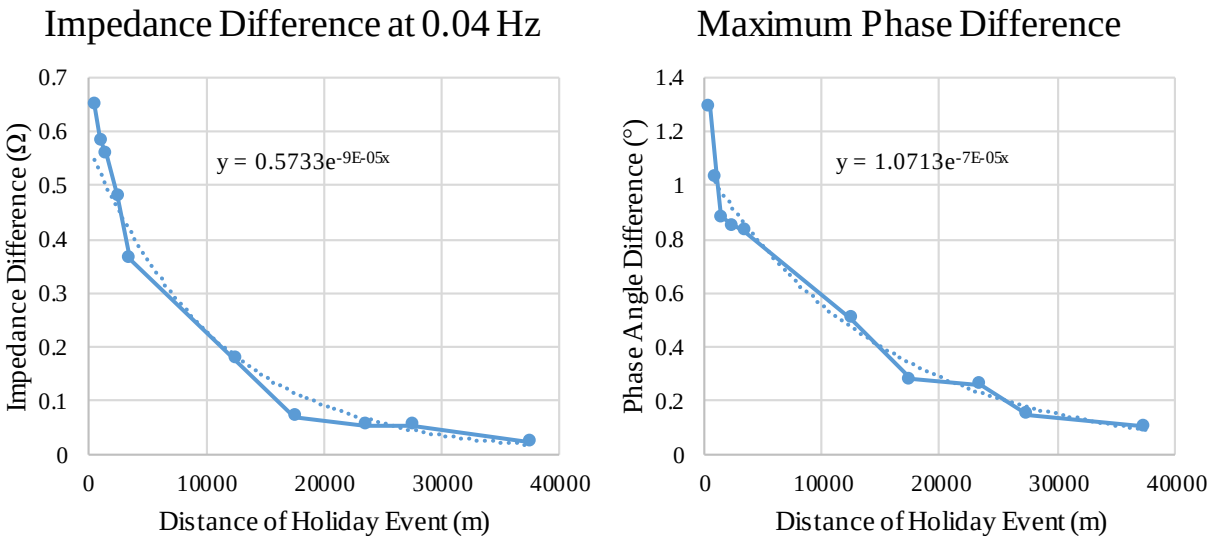

Figure 19: Impedance and phase difference profiles with varying distance to holiday defect

It has been shown that impedance spectroscopy is susceptible to pick up the effect of a relatively small coating defect very far from the measurement point, as shown on figure 18 and 19, and provide information on either the size or the location of the defect. However, given the need to compare the results with the those of the same structure or pipeline with an intact condition, it would only be suited for monitoring purposes.

These results have lead the author of this thesis to push research further into a technology that would be able to overcome this limitation.

Transmission line theory

The transmission line theory covers the modelling of long, parallel conductors. The configuration of these parallel conductors induces a coupling of the electromagnetic waves travelling in these conductors, and this coupling and the properties that ensues is the object of study of transmission line theory. Historically, it has been used extensively for phone and power lines [1].

The central definition and property of a transmission line is the one of characteristic impedance. In a transmission line copmrising two parallel conductors characterized by a inter-conductors lineic capacitance C, a lineic inductance L, a lineic resistance R, and a lineic conductance G, as represented in Figure 20, we define its characteristic impedance as follow:

$$Z_C = \sqrt{\frac{R + jL\omega}{G + jC\omega}} \qquad (2)$$

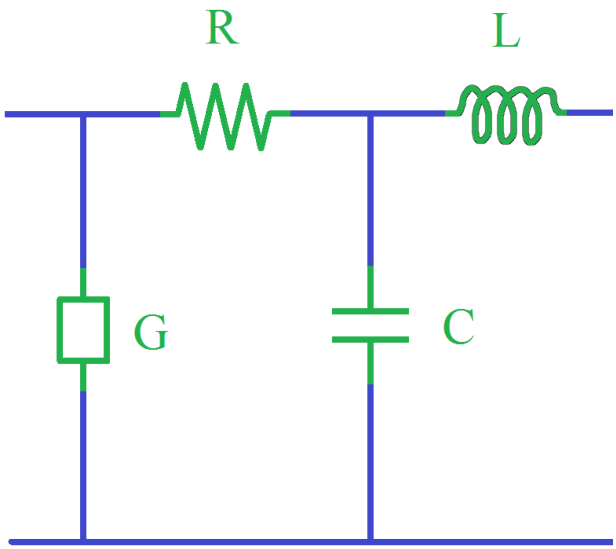

Figure 20: Lumped lineic elements of a transmission line

The principle of reflectometry is to study the reflections of a known signal sent into a medium to gather information on the spatial disparities of physical properties within this medium. The most famous application of reflectometry is probably the RADAR (Radio Detection And Ranging) system, which uses radio waves in the atmosphere.

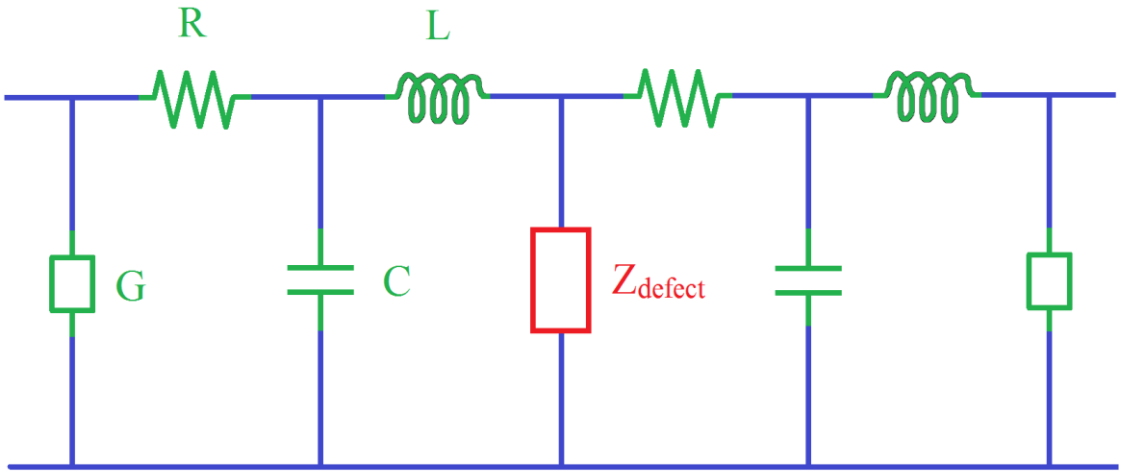

Figure 21: Transmission line with a shunt defect across the two conductors

Transmission lines happen to be extremely well suited for reflectometry of electrical waves [2]. Given that a transmission line has a reasonable attenuation and distortion coefficients, a signal can travel forth and back for miles. Any change in the characteristic impedance of the line, and any discontinuity such as a shunt across the two conductors will induce a reflection. Since the reflected wave travels at the same speed as the incoming wave, the location of the discontinuity can be computed.

In the case of a shunt across the two conductors as illustrated in Figure 21, the magnitude of the reflected wave is defined as follows:

E_i	Incoming voltage
E_r	Reflected voltage
Γ	Reflection coefficient
Z_c	Characteristic impedance of the line
Z_{defect}	Impedance of the shunt across the two conductors

$$\Gamma = \frac{E_r}{E_i} \quad (3)$$

$$\Gamma = -\frac{Z_C}{Z_C + 2\,Z_{defect}} \quad (4)$$

The litterature about the application of transmission line theory to a pipeline system is extremely limited, and this for a simple reason: the difficulty lies in the definition of the system. In "Simulation of Pipeline Holiday Detection by Time Domain Reflectometry" by Zsigmond and Johnston [3], old and debatable models of the current distribution in the ground [4] have been used to define a system with one pipeline as one conductor, and the surrounding ground as the other conductor.

This definition makes the computation of the line parameters open to controversy, and leaves plenty of room for doubt regarding its field application. But most importantly, it does not solve the question of the baseline. Reflectometry profiles of complicated systems, such as a real pipeline layout, have to be compared to a baseline in order to be used efficiently, and that often proves to be a major shortcoming [5]. Such a system does not provide a baseline, unless used as a monitoring system.

The author of this thesis leaves to the reader to read this Zsigmond and Johnston paper to further understand the shortcomings of that approach.

CHAPTER III

APPLICATION OF REFLECTOMETRY FOR PIPELINES

The three-media transmission line

We have reviewed in the previous part the basic theory for reflectometry, and we have seen that its application to a pipeline system is non-obvious. Indeed, the study of classical transmission line theory (references), and the review of the limited existing literature drew the author to the conclusion that the simple system of one pipeline (as

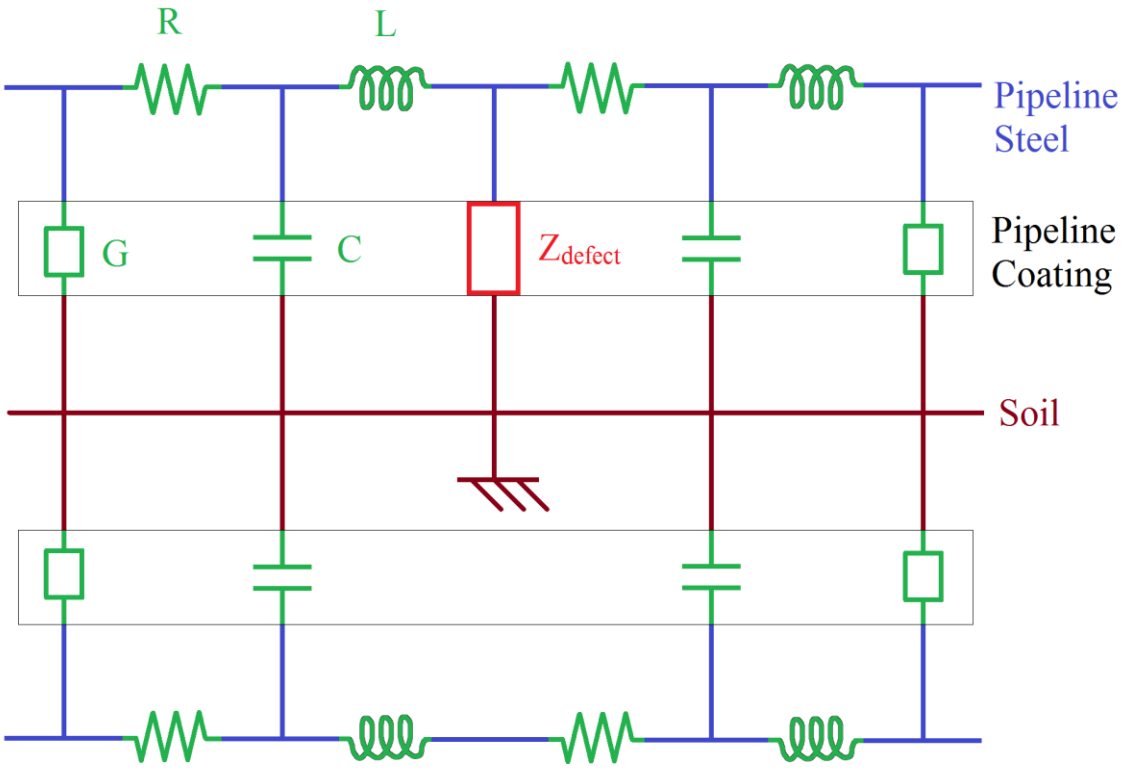

Figure 22: The three media transmission line

signal-carrying medium) and the neighboring soil (as return path), was ill-suited for practical purposes application of reflectometry.

Scientific intuition has led the author to think that it was needed to vastly increase the quality of the transmission line considered, at the expense of the hardness of the reflections. This goal has been achieved by working within a novel paradigm for reflectometry, with the use of a three-media transmission line: one pipeline as signal-carrying medium, another pipeline as return path, and the soil as the reference potential to which coating defects act as shunt impedances (see figure 22).

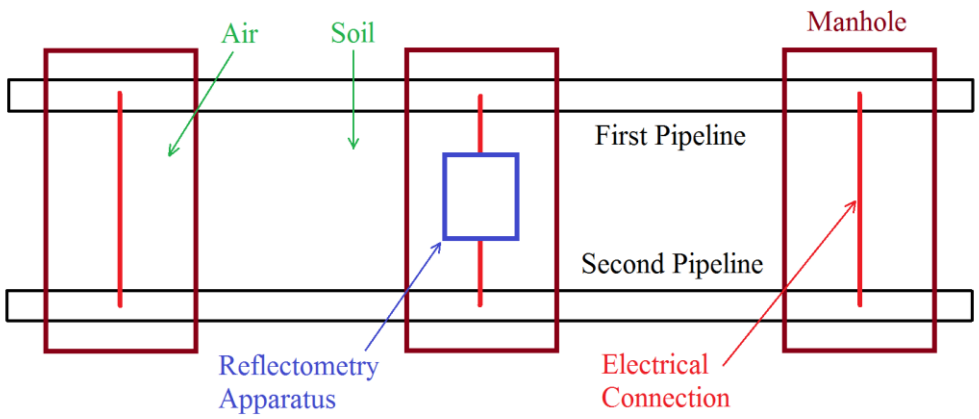

Figure 23: Field application framework

It is interesting to precise here a framework for field application of this paradigm that has been deemed particularly useful and practical: buried pipelines are most often accessible at regular locations, called manholes, that are small concrete structures that allow operators to go down at the depth of the pipes. In order to share the cathodic protection among those pipes, they are usually all connected together with copper cables.

Technically, this makes a set of three adjacent manholes a simple and efficient framework, with the reflectometry apparatus installed at the manhole in the middle, where the cables connecting all pipes together have been severed and used to connect the reflectometry apparatus, as shown in Figure 23.

Within this framework, the configuration of the pipelines and the system beyond those three adjacent manholes is effectively ignored because of the shortcut, or closed termination of the transmission line on both sides.

Classical reflectometry has a terminology convention: reflections due to open-circuit terminations, short-circuit terminations, or small shunt impedance discontinuities across the line all have strong signatures and hence are called "hard" reflections. On the contrary, other minor reflections, typically, for example, a coating defect for a wire in air, have much weaker signatures and are called "soft" reflections and can be extremely hard to detect [6].

Within the three-media transmission line paradigm, the kind of reflections that defects in the coating of the signal-carrying pipeline induce are, stricto sensu, neither hard nor soft reflections. Indeed, those reflections are induced by a current transfer from one conductive medium (the steel of the pipeline) to another (the soil), but this other medium is technically not the signal returning medium. These reflections have high amplitude, like hard ones, but they are much less sharp. We named those "third medium" or "soil" reflections. In order to illustrate those differences, a simple electric experimentation has been designed.

A 50 Ω RG-58U coaxial cable, i.e. a transmission line with a characteristic impedance of 50 Ω for radio frequencies (in the frequency range used for reflectometry this impedance is slightly higher due to the influence of the lineic resistance term in equation (2)) is used. An adaptable resistance is used as shunt.

In the case of the hard reflections set up, this resistance is shunting directly the inner conductor of the cable with the outer conductor. In the case of the soil reflections set up, the resistance is shunting the inner conductor with the earth. In both cases, the shunt is located at the end of a 48 feet long coaxial cable to the oscilloscope, and then followed by another 48 feet long coaxial cable terminated by its characteristic impedance. Both setups are shown with both a visual and an electrical illustration, as shown on figures 24 to 27.

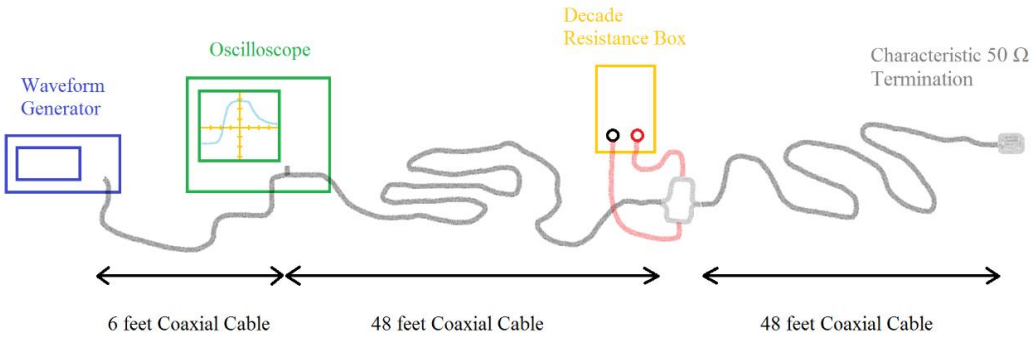

Figure 24: Hard reflection setup illustration

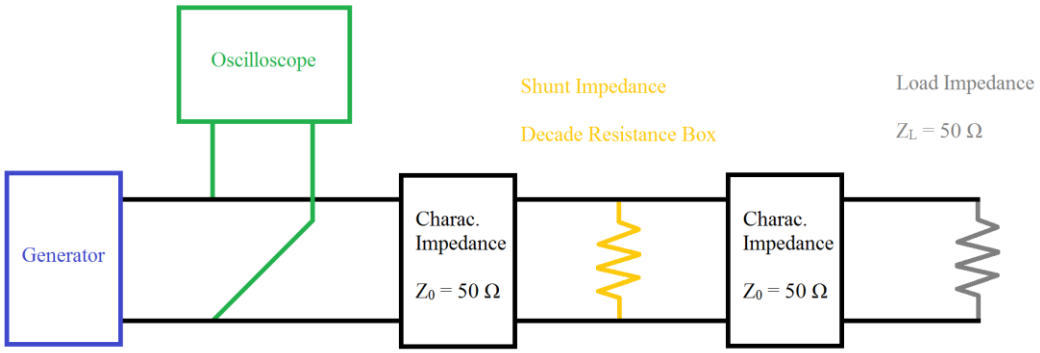

Figure 25: Hard reflection setup electrical layout

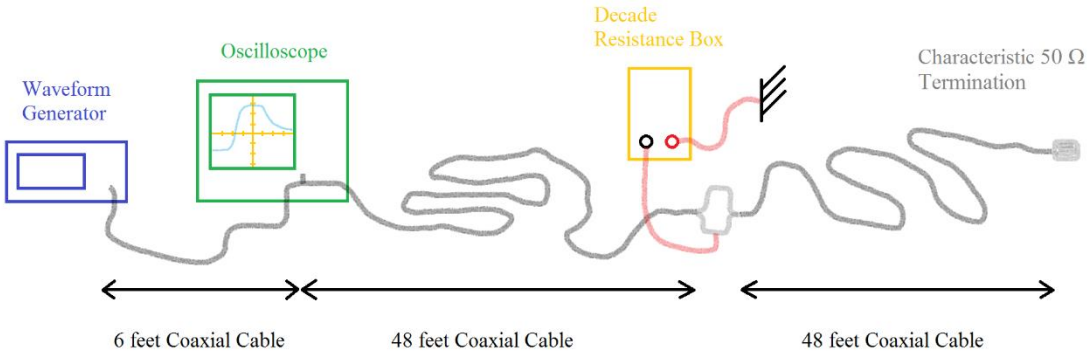

Figure 26: Soil reflection setup illustration

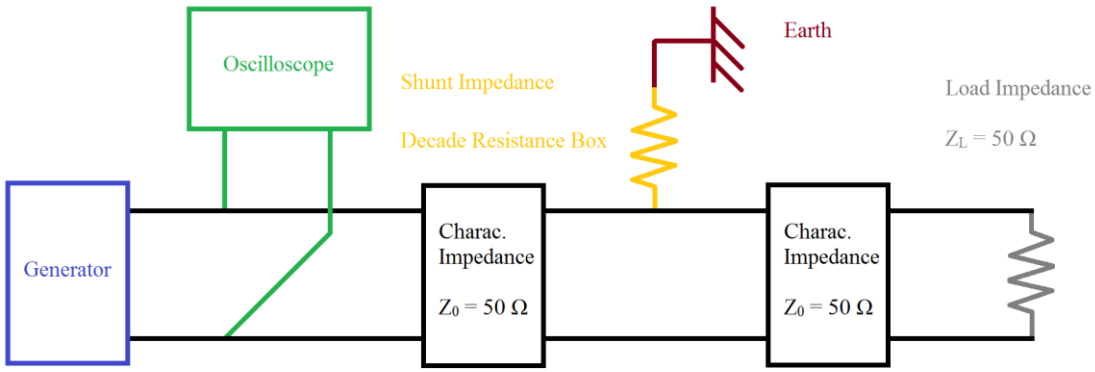

Figure 27: Soil reflection setup electrical layout

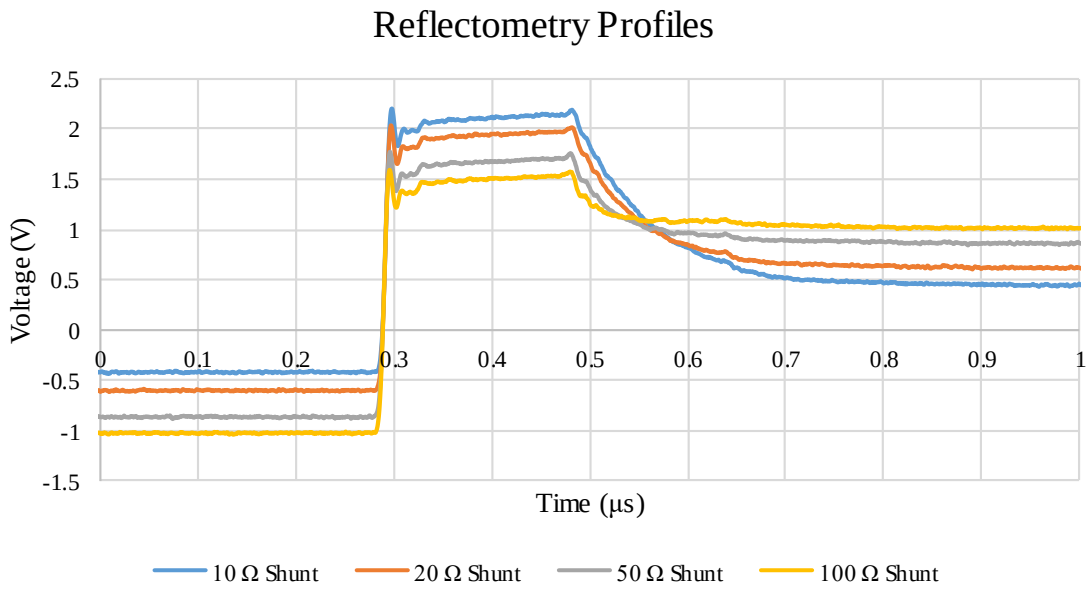

Figure 28: Reflectometry profiles for the hard reflections setup

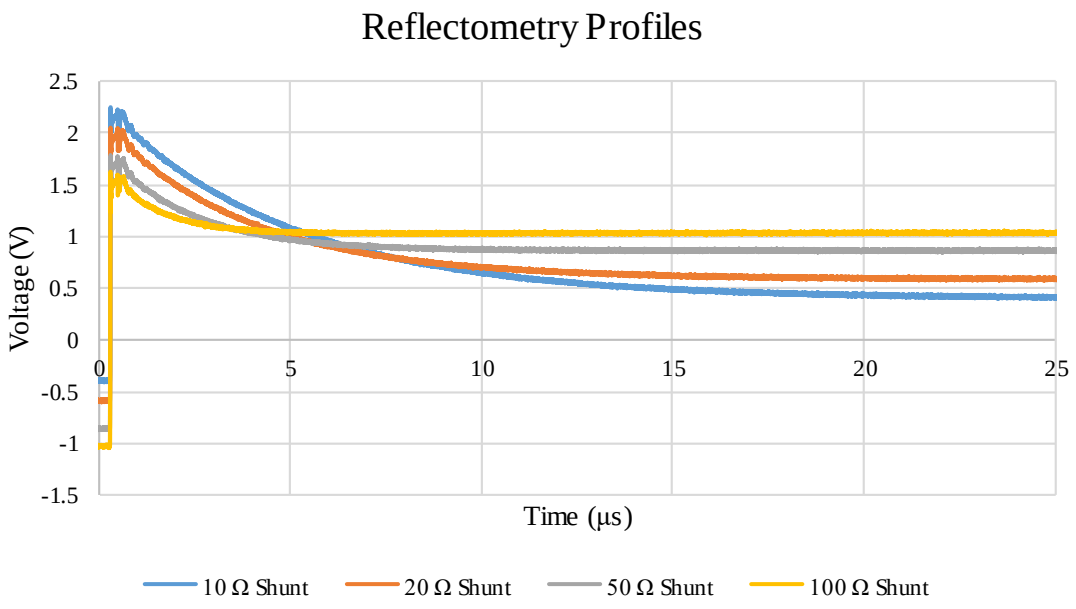

Figure 29: Reflectometry profiles for the soil reflections setup

It is readily observable in Figures 28 and 29 that the amplitude of the reflections are the same for both set up, and that the difference lies in the sharpness of those reflections. Both types of reflections appear to be exponential steps, which we can modelled with the following formula:

$$E(t) = E_i\left(1 - \Gamma e^{-\frac{t}{\tau}}\right) \qquad (5)$$

With τ, the time constant, being significantly larger for soil reflection than for hard reflections 1. The interpretation of these results is the following: for hard reflections, the transformation of the "clean" voltage step into an exponential step is due to the distortion of the line. Indeed, we know with Fourier's series that a step signal is nothing else than a

sum of sine signals of different amplitudes and frequencies. And real transmission lines are not ideal and have their characteristic impedance that depends on the frequencies, hence distorting the signal.

For soil reflections, the understanding of the author is that a soil reflection is akin a negative current step input for the system, as current flows out of the conductor into the soil and that therefore its answer obeys a time constant just like a classical RLC (resistance-inductance-capacitance) system does.

Laboratory results

It has been found that the signal, i.e. the voltage difference between the two pipes (or inner and outer conductor) is affected by reflections only by defects in the coating of the signal-carrying pipe or conductor. Hence, on a symmetrical electrical layout, such as two parallel pipes, it is possible to extract meaningful data by comparing the reflectometry profiles obtained by two different configurations, that differ only by the polarity between the two conductors, i.e. which one is the signal-carrying conductor and which one is the "return" conductor.

In order to illustrate these explanations, Figures 30 and 31 show screenshots from oscilloscope readings of a laboratory simulation of two parallel pipelines, in the same laboratory simulation system of NS4 (a solution designed to mimic soil properties), one intact and one with a delamination defect (2 $inch^2$), and ended with the characteristic impedance of the line

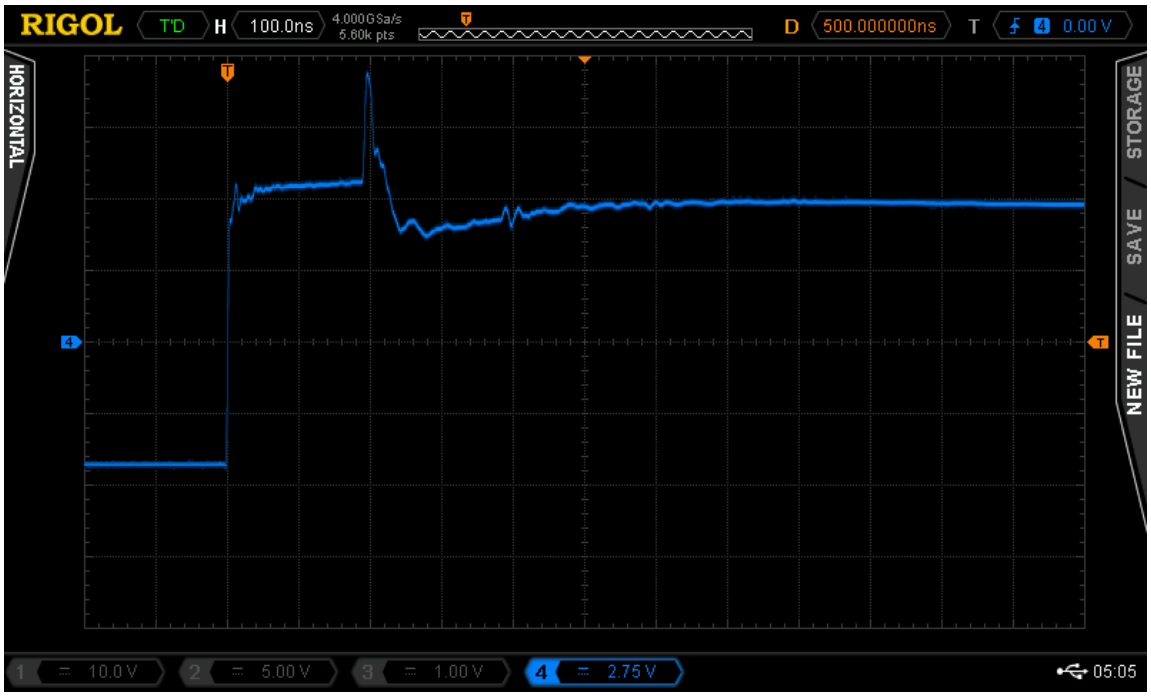

Figure 30: Profile with intact pipe carrying the signal

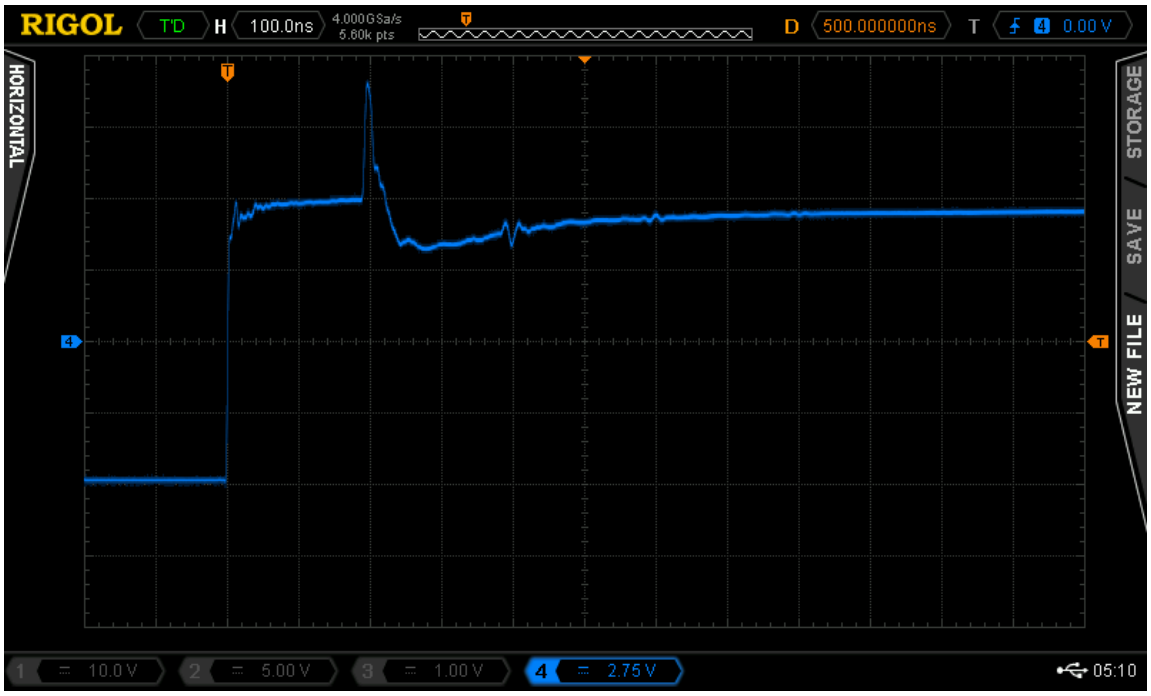

Figure 31: Profile with intact pipe returning the signal

It can be seen on those screenshots that many unwanted reflections (for coating assessment purposes) are occurring, including those due to the cable-to-pipe welds, the air/NS4 solution change of electrical permittivity, and coaxial cable/copper wire, and copper wire/steel pipe impedance mismatch. Hence, the study of only one of this plot is difficult. The comparison of those plots however, i.e. subtracting one profile to the other, given the transversal symmetry of the problem, yields very good results regarding the characterization and localization of the defect, as illustrated in Figure 32.

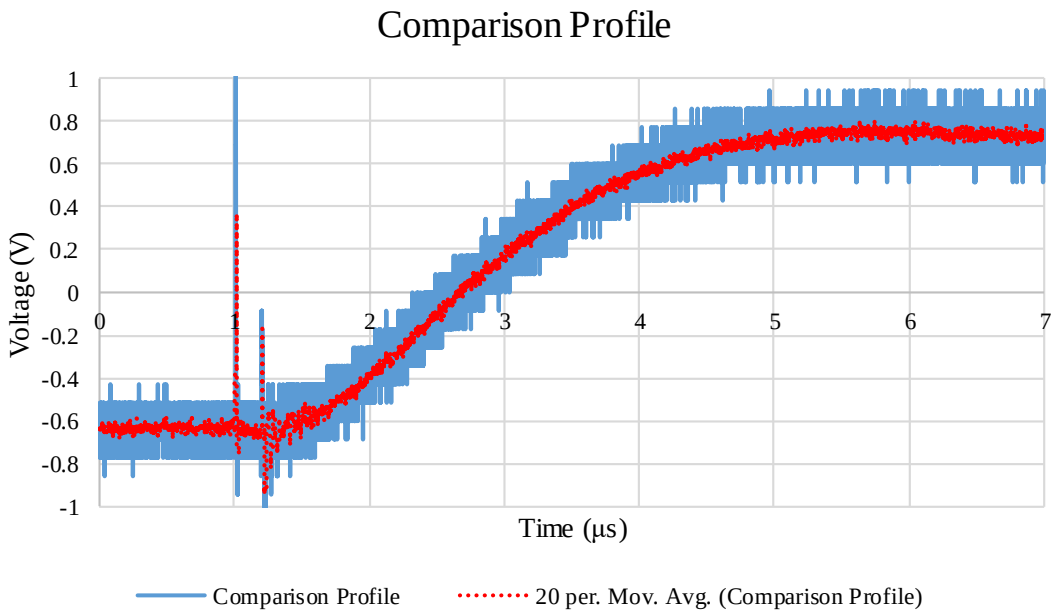

Figure 32: Comparison of the two reflectometry profiles of symmetrical configurations, terminated with the characteristic impedance of the line

These results are coherent with the conclusions drawn on purely electrical simulations and testings regarding the characterization of soil reflections induced by coating defects.

CHAPTER IV

FIELD CONSIDERATIONS AND RESULTS

Critical analysis of the DCVG/CIPS method and sensitivity comparison with reflectometry

The DCVG (Direct Current Voltage Gradient) method is an approach designed to locate defects in a pipeline coating. It is local in the sense that it requires one or a team of operators to survey the whole distance on top of the pipeline with closely-spaced potential measurements.

This technique can be used longitudinally or transversally, depending on whether the voltage gradient measured is parallel or perpendicular to the axis of the pipeline.

The most practical to perform such a survey is to use metallic poles, similar to hiking sticks, as ground electrodes. Hence, with one pole in each hand, one operator can measure a potential difference in the ground within his arm span. In the vicinity of a defect in the coating of the pipeline, the cathodic protection applied to the pipeline, leaking through the defect, is a current source and the gradient measured is an ohmic voltage drop in the ground, as shown in Figure 33.

It is a reasonable assumption to deem the equipotential surfaces in the soil to be spherical at some distance of the defect [7]. Let us proceed to some resistance considerations in the soil within this framework.

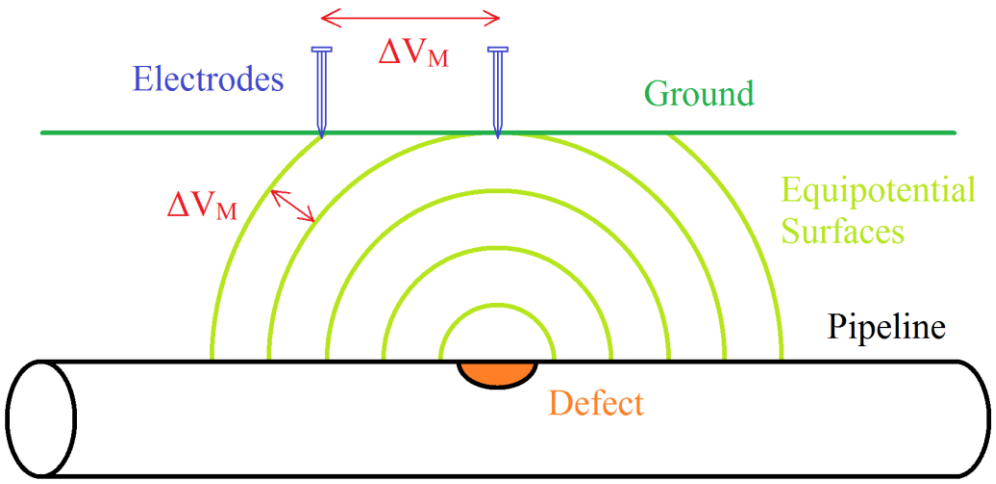

Figure 33: DCVG principle illustration

First, we define the concept of resistance (or impedance) to close earth R_{CE} as the resistance (or impedance) met by current flowing from the steel of the pipe to a spherical surface centered on the pipe at the defect location, through the defect in the coating. Typically, owing to the laboratory set up with which we worked for EIS (and the distance at which counter electrodes were placed), here for the sake of our example we define the radius r_{CE} of such a sphere as 20 cm. For a point further away from the center of the pipe than this radius, the resistance met by current flowing from the pipe steel to this point can be seen as the sum of two terms, R_{CE} and $R(d)$, $R(d)$ being the distance dependent term, and within our framework it can be calculated as the resistance met by current flowing from a sphere surface of radius r_{CE} to a radius d. Hence:

$$R(d) = \int_{r_{CE}}^{d} \frac{\rho}{4\pi r^2} dr \qquad (6)$$

In order to evaluate the potential induced by the leaking of the voltage applied to the pipe at any point in the ground, we can see the system as a simple series circuit between the steel of the pipe and the remote earth, as shown on illustration n. We can define R_{RE}, the resistance met by the current flowing from the steel of the pipe to remote earth as:

$$R_{RE} = R_{CE} + R(d = \infty) \qquad (7)$$

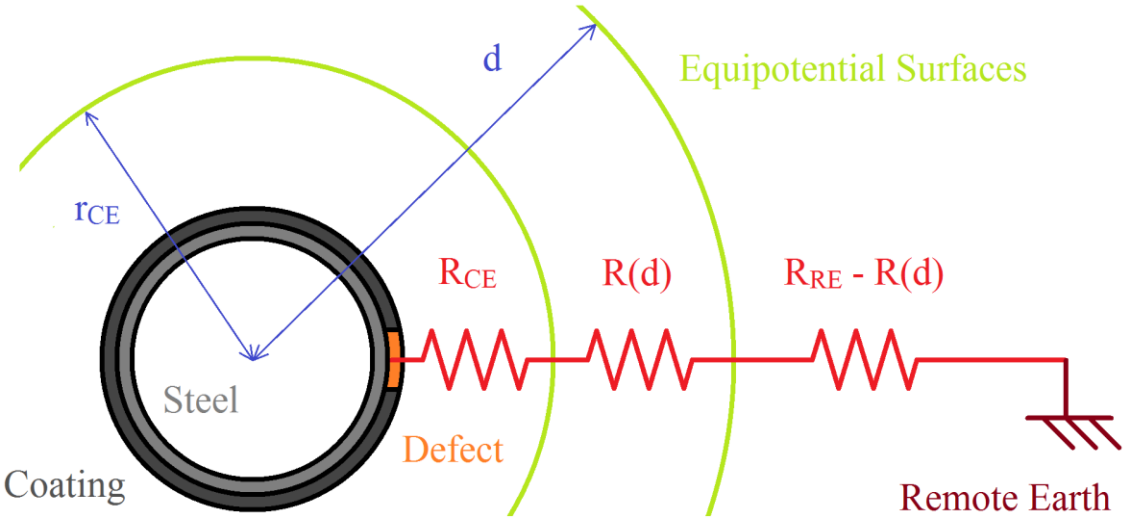

Figure 34: Soil electrical modelisation illustration

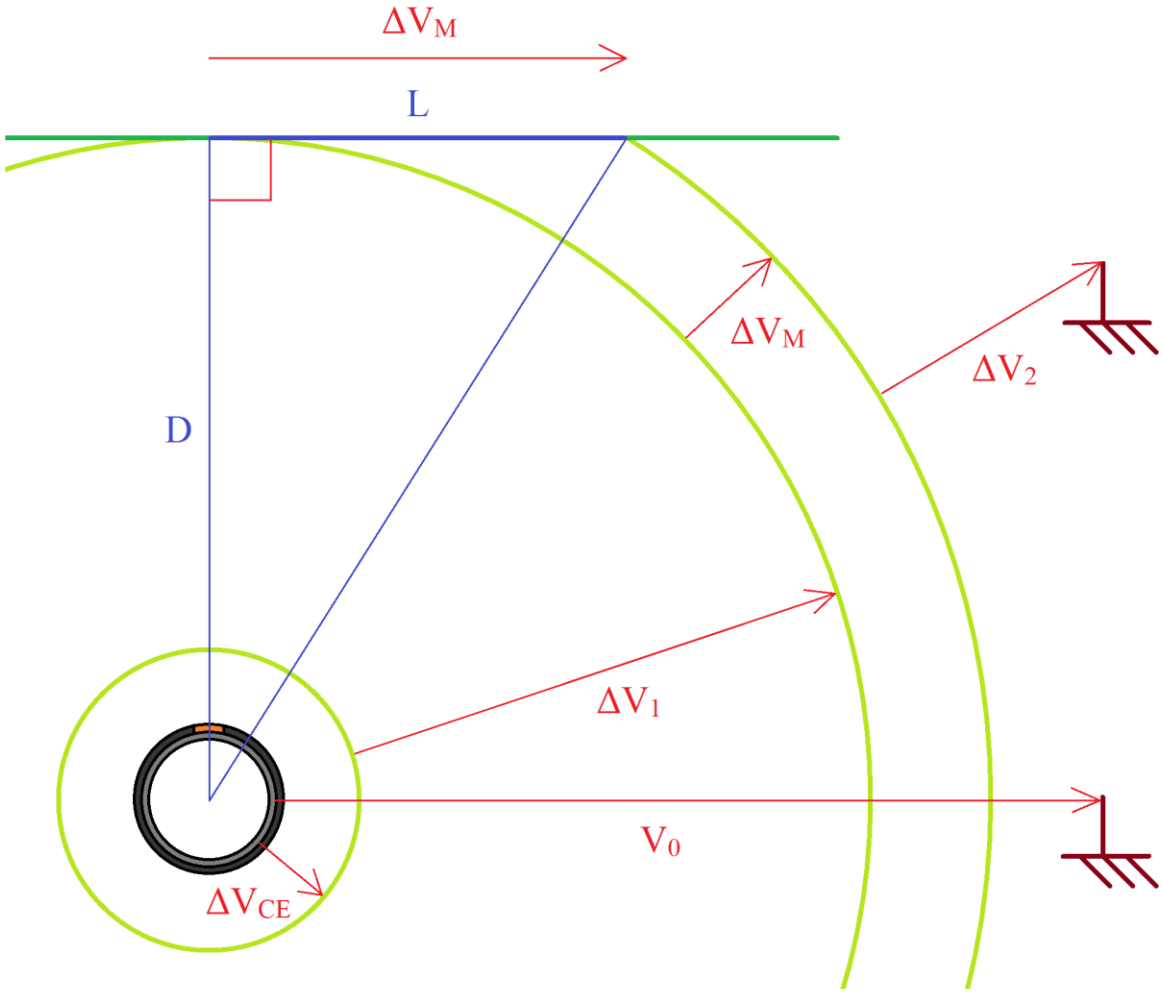

Figure 35: Potential differences in the soil illustration

Let us define V_0 the potential of the steel at the defect location.By definition, the potential of remote earth is zero. According to the well-known Ohm's law, ΔV_M, the voltage that is measured by the DCVG method is only a fraction of V_0, as shown on figure 35.

$$\frac{\Delta V_M}{V_0} = \frac{R\left(\sqrt{L^2+D^2}\right)-R(D)}{R_{RE}} \quad (8)$$

$$R\left(\sqrt{L^2+D^2}\right) - R(D) = \int_D^{\sqrt{L^2+D^2}} \frac{\rho}{4\pi r^2}\, dr \quad (9)$$

$$R_{RE} = R_{CE} + \int_{r_{CE}}^{\infty} \frac{\rho}{4\pi r^2}\, dr \quad (10)$$

In fine, we have for DCVG:

$$\frac{\Delta V_{M,DCVG}}{V_0} = \frac{\frac{\rho}{4\pi}\left(\frac{1}{D}-\frac{1}{\sqrt{L^2+D^2}}\right)}{R_{RE}} \quad (11)$$

And for reflectometry:

$$\frac{\left|\Delta V_{M,Reflectometry}\right|}{V_0} = \frac{Z_0}{Z_0+2R_{RE}} \quad (12)$$

The dependence of this sensitivity ratio to the parameters D, L and ρ has been investigated (Figures 36, 37, 38, 39). The standard value of 1.5 m (~5ft) used for L is the one recommended by most manuals [8], however on the field, operators have to perform hundreds or thousands of measurements and tend to maintain a more comfortable position with their arms, which therefore leads to a smaller span L for the voltage measurement,

typically about 0.6 m (~2ft). This reduces further the sensitivity of the DCVG method, as illustrated in Figures 37 and 38.

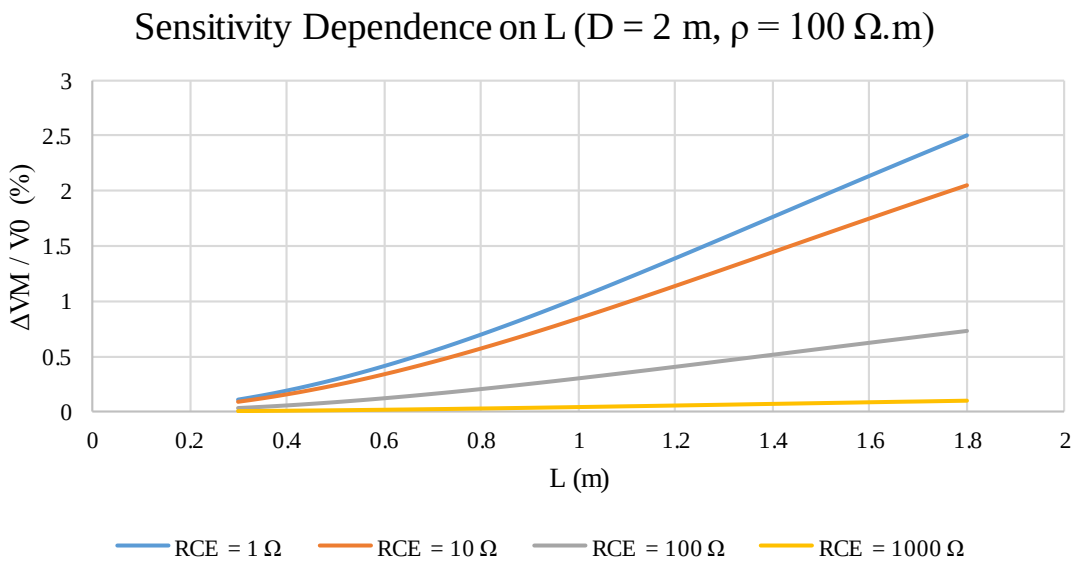

Figure 36: Sensitivity Dependence on L for the DCVG method

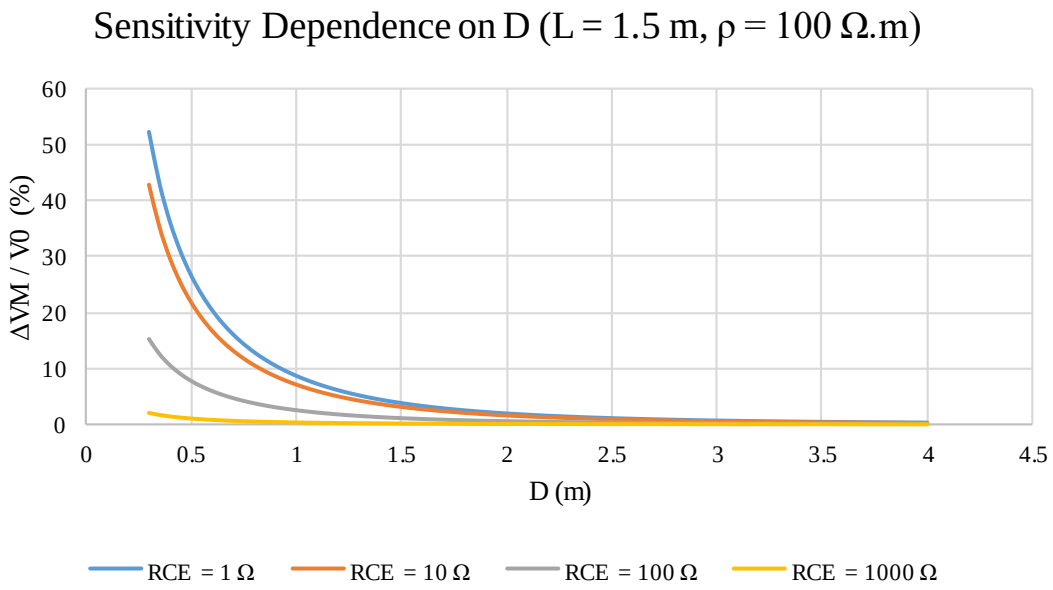

Figure 37: Sensitivity dependence on D for the DCVG method

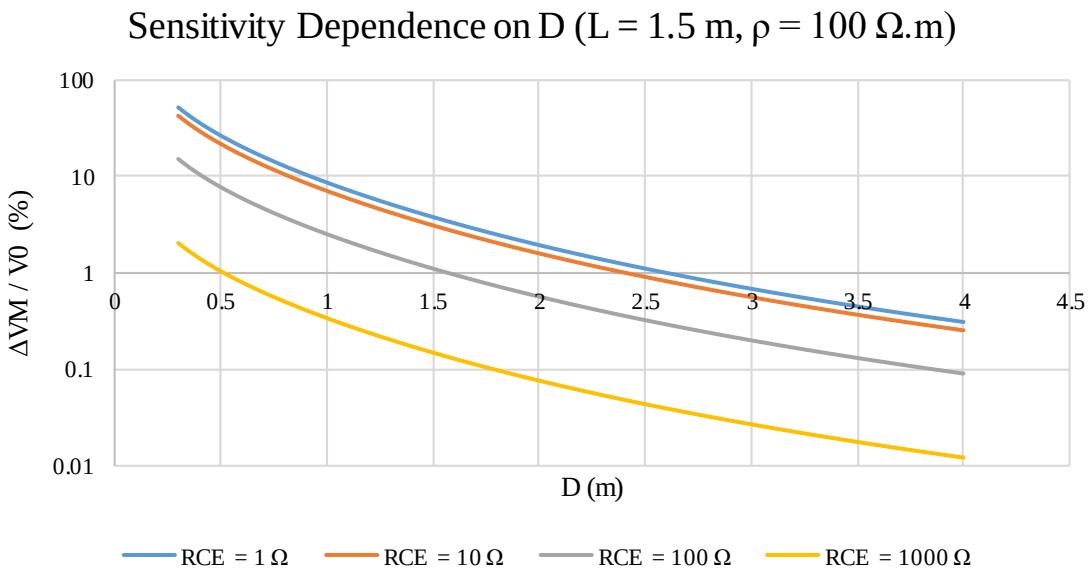

Figure 38: Sensitivity dependence on D for the DCVG method (logarithmic scale)

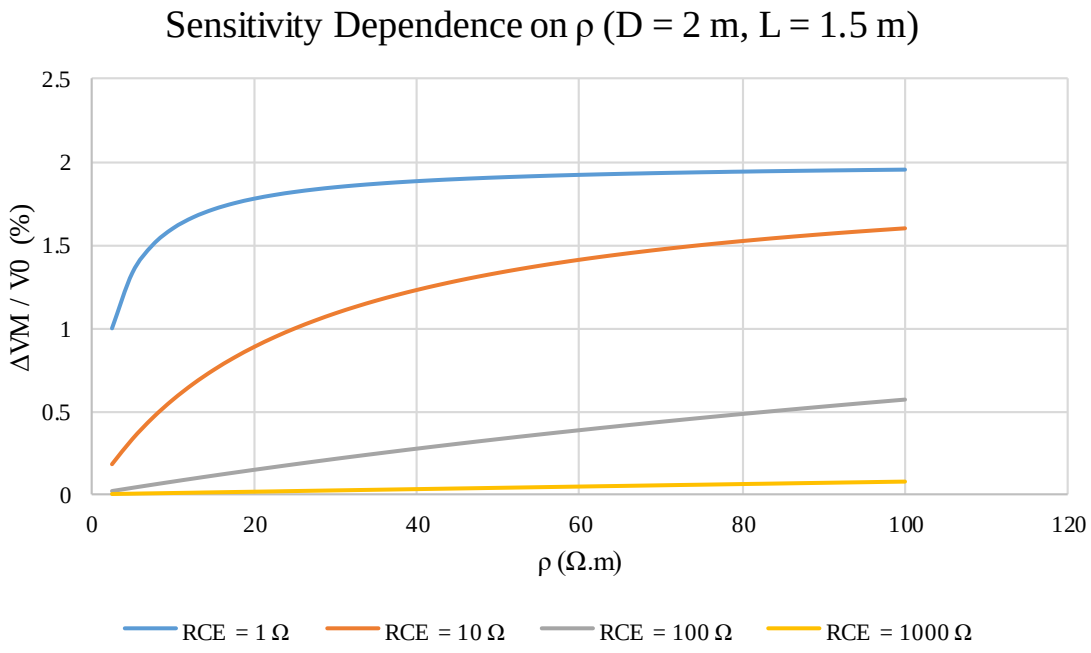

Figure 39: Sensitivity dependence on ρ for the DCVG method

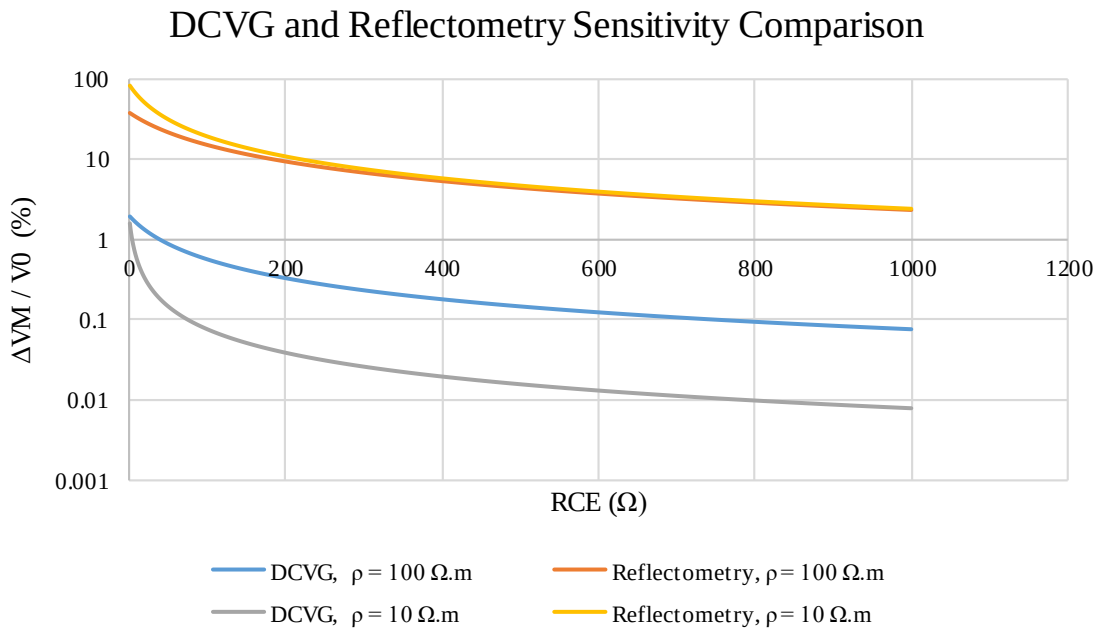

Figure 40: Sensitivity dependence on defect impedance for both the DCVG and the reflectometry methods

This strong dependency on soil resistivity for DCVG can been considered as an inherent flaw, as low soil resistivities are associated with high corrosiveness, as shown on the table 4 from the British Standard BS-1377.

Table 4: British Standard BS-1377

Soil Resistivity ρ	**Soil Corrosiveness**
$\rho > 100\ \Omega.m$	Slightly Corrosive
$50\ \Omega.m < \rho < 100\ \Omega.m$	Moderately Corrosive
$10\ \Omega.m < \rho < 50\ \Omega.m$	Corrosive
$\rho < 10\ \Omega.m$	Highly Corrosive

The most used protection criteria is the – 850 mV (CSE) potential criterion. In the NACE standard SP0169, it is defined as follow in paragraph 6.2.2.1.1 [9]:

> *A negative (cathodic) potential of at least 850 mV with the cathodic protection applied. This potential is measured with respect to a saturated copper/copper sulfate reference electrode contacting the electrolyte. Voltage drops other than those across the structure-to-electrolyte boundary must be considered for valid interpretation of this voltage measurement.*

This formulation clearly states that ohmic drops (that include ohmic drops in the ground) have to be taken into account to use correctly this criterion. However, the current practices of many corrosion services companies using CIPS/DCVG is to compare the potential measured on the surface of the ground to the potential of the voltage delivered by the rectifier. The very fact that soil resistivity is a critical factor for the determination of soil corrosiveness provides strong support to the claim that this NACE cathodic protection criteria is widely misused in the field application of the CIPS method.

Field results

Field testings have been conducted in New-York City with 12 inch coated steel pipeline networks and assets between November 2016 and September 2017.

Parallel conductors transmission lines are suited to both grounded signals and differential signals. Hence differential signals, where both pipes carry opposite potentials, have also been used in field conditions.

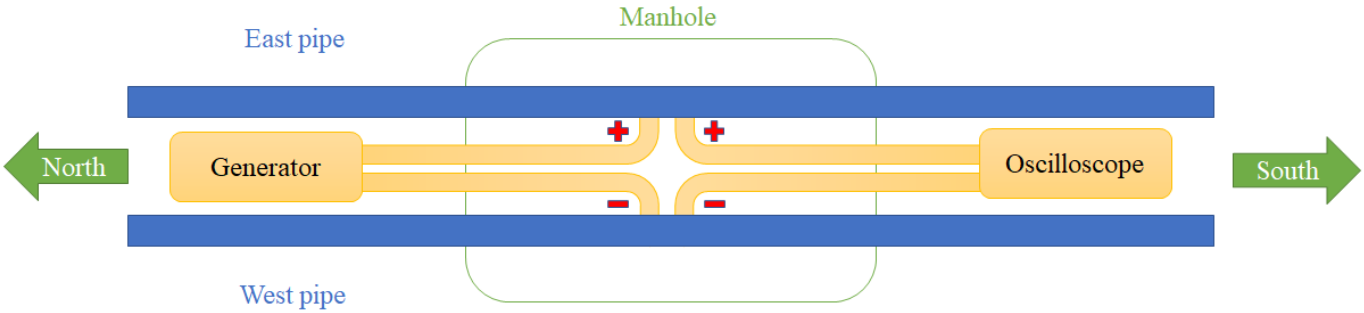

Figure 41: Basic set up framework within a manhole

The standard operating procedure that was followed on these pipeline assets includes pumping out the water accumulated in the manhole, lifting the cathodic protection bondings from the pipes, stripping the coating off both pipes over a small area, cleaning it with alcohol, connecting the hardware, and checking the resistance of each of those connection points. The crew got used to call those connection points "patches".

Figure 42 is the reflectometry profile, using a differential square signal, obtained at a manhole located close to Harlem River.

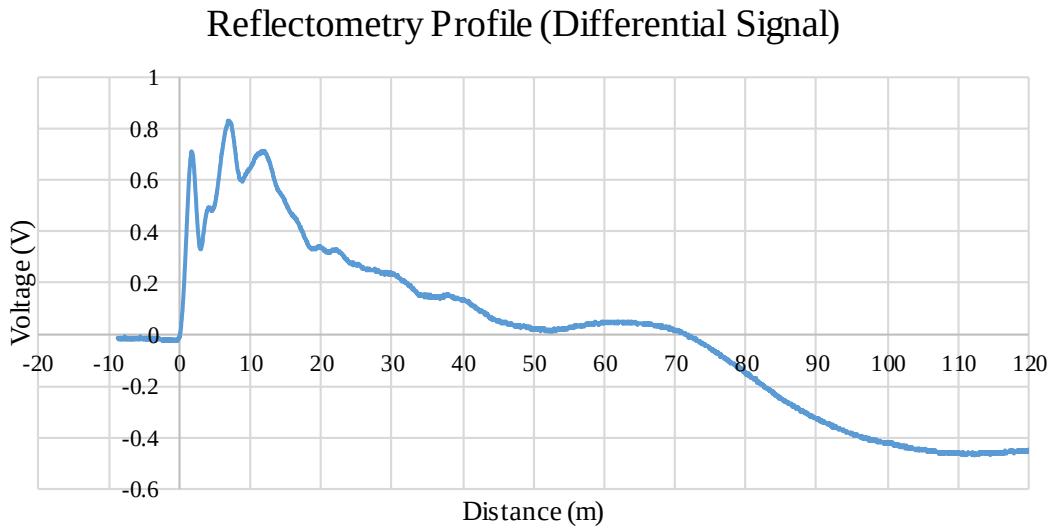

Figure 42: Reflectometry profile at the Harlem River location (differential signal)

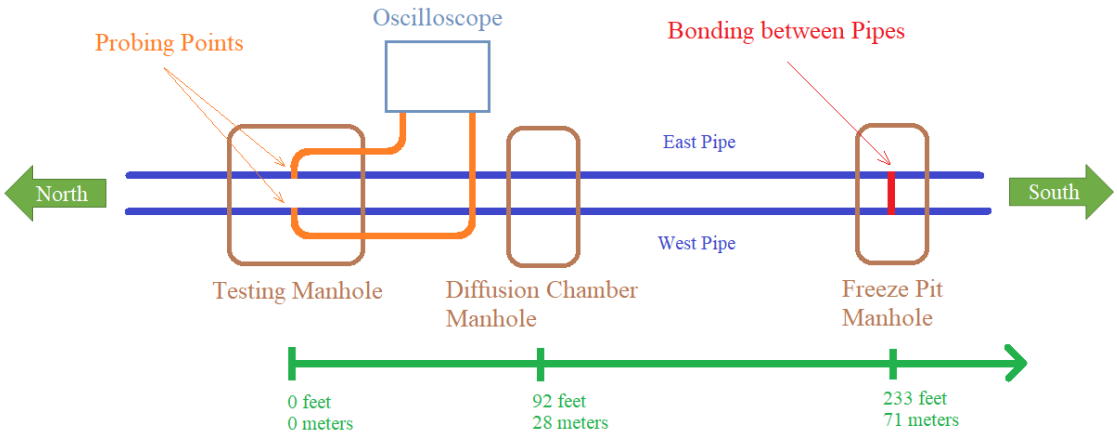

Figure 43: Layout of the system on the southern side of the Harlem River location

Soil reflections cannot drive the voltage read by the oscilloscope across the pipe below zero, i.e. invert the potential polarity that was applied to those pipes with the square signal from the waveform generator. A hard reflection from a bonding between both pipes, however, can. This profile is therefore useful; first to check the coherence of the calculated speed of the signal, i.e. as a distance calibration, and second to evaluate the signal attenuation and distortion. It is a reasonable assumption for field application that the voltage evolution read between 70 and 110 meters are entirely due to this inter pipes bonding at the freeze pit manhole. Indeed, the very large amplitude of the reflections experienced closer to that distance suggest that those occur on the northern side of the manhole, where half of the signal went, which means that large coating defects exist on both pipes (East and West) within 10 and 40 meters, and that those defects are large enough that there is not much left of the signal amplitude to travel on the northern side beyond that distance.

We determined that the amplitude of the freeze pit bonding reflection is 500 mV, and this value is proof of reasonable attenuation from both travel within the transmission line defined by both parallel pipelines itself and reflections at the air/soil and soil/air interfaces met along the way, given the very challenging layout of this location. The same reasoning holds true for the distortion of the signal: instead of being a very sharp reflection, with a rising time of a few tens of nanoseconds, the reflected wave spreads over 1.6 μs (equivalent time to travel 40 m), which is also a reasonable value of signal distortion given that it travelled through no less than 4 air/soil and 4 soil/air interfaces.

Furthermore, this location being very close to the Harlem River, and free of concrete, the soil has been found to be comparatively very wet (about 30% humidity) which means higher dielectric permittivity difference between the soil and air. In other (drier) locations, like in Manhattan or in the Bronx where the ground is completely covered in concrete, those dielectric permittivity discrepancies have been found to be smaller and hence distortion milder.

The author of this thesis invites the reader to compare the reflectometry profile of this Harlem River location to the profile obtained in a Bronx manhole, as illustrated in Figure 43. At this Bronx location, there is no manhole other than the one used for the testing in the vicinity of the measurement.

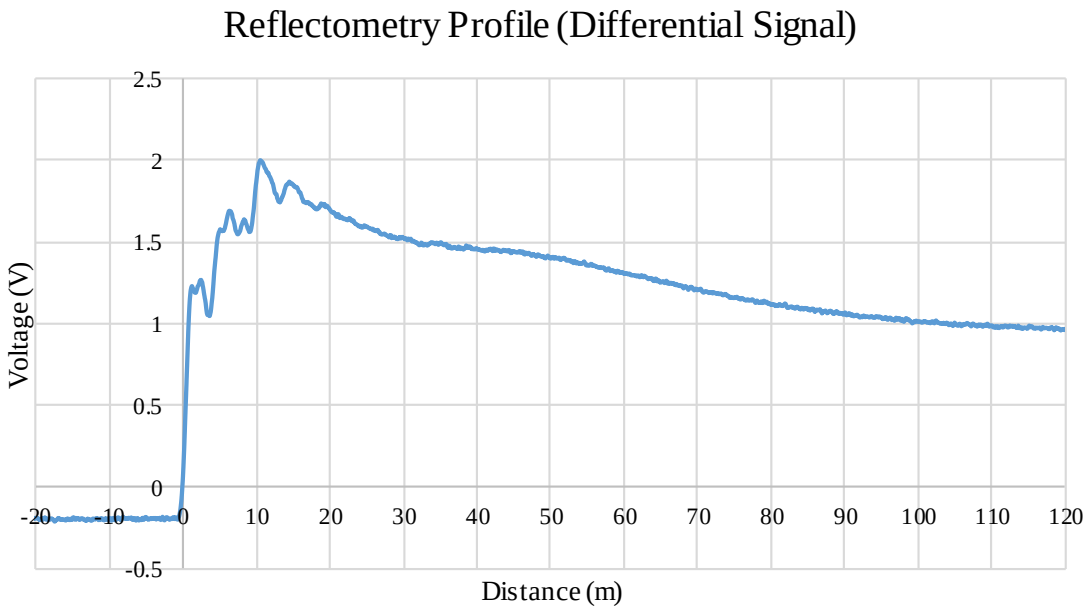

Figure 44: Reflectometry profile at the Bronx location (differential signal)

We observe that, contrary to Harlem River location, the signal remains relatively strong and experiences fewer reflections. Specifically, it remains stable beyond 120 m. It appears that two large reflections can be attributed to coating defects, around 20 m and around 50 m.

Further interpretation requires the use of grounded signal, and the west pipe, east pipe and comparison profiles that come from it (when respectively the west pipe or the east pipe carry the signal voltage).

Multiple setups regarding the positioning of the connection points of the oscilloscope probe and the generator output have been used. Specifically, with four connection points or patches made on the northern and southern ends of the manhole, on both pipes, all four possible combinations of positioning for the oscilloscope probe and generator output have been carried out, as schematized on Figures 45 to 48.

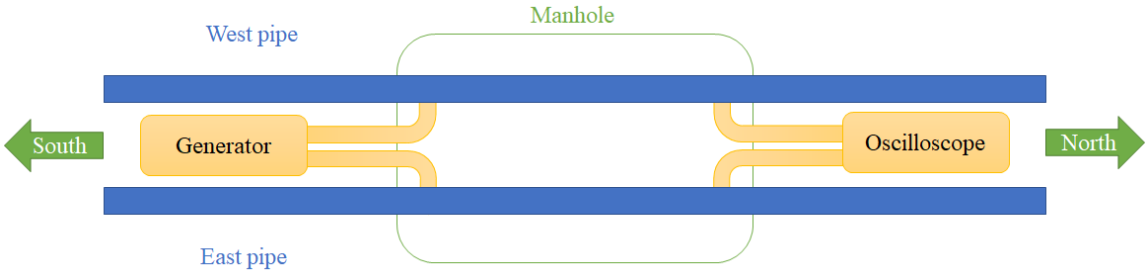

Figure 45: Generator South, Oscilloscope North setup (GSON)

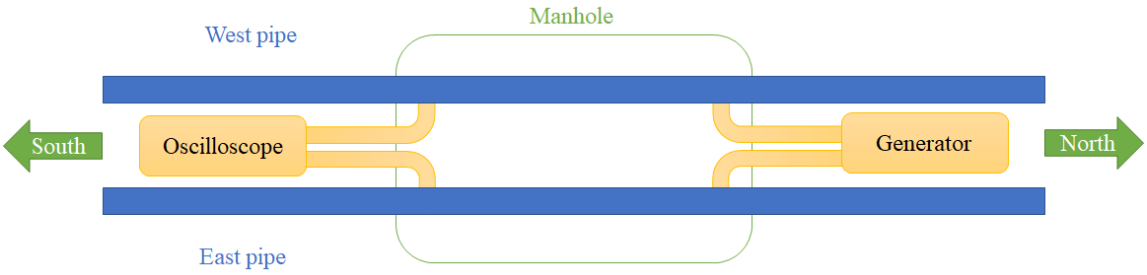

Figure 47: Generator North, Oscilloscope South setup (GNOS)

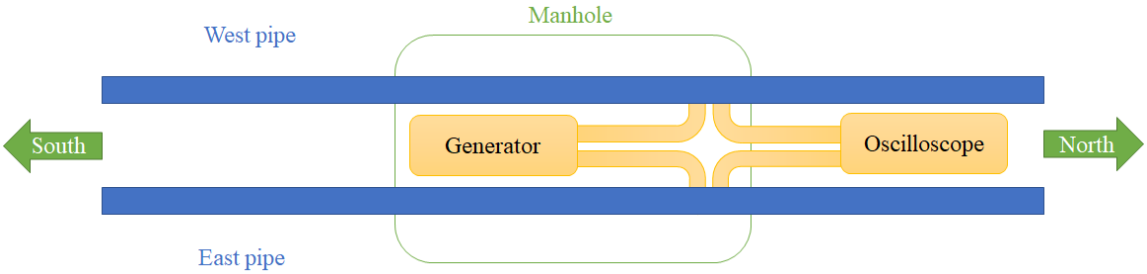

Figure 48: Generator North, Oscilloscope North setup (GNON)

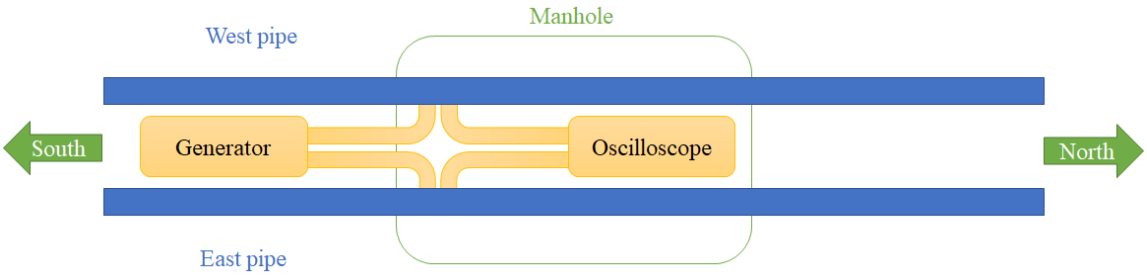

Figure 46: Generator South, Oscilloscope South setup (GSOS)

Both "trans" configurations (GSON and GNOS) and "cis" configurations (GNON and GSOS) have different complementary advantages. In trans configurations, intra manhole ringing is reduced since the first air/soil interface reflection is screened due to the location of the probing points. However, trans configurations do not allow to determine the direction of the defects detected. Indeed, the signal shoots on both directions, and comparison between the GSON and the GNOS does not allow to extrapolate the direction

since both configuration have the same effective signal travel time. Determination of the direction of the defects detected is achieved with cis setups, since defects seen on the GSOS profile will be seen with either a lag or an advance on the GNON profile, depending on whether those defects are located on either the northern or the southern side of the manhole (Figures 49,50,51).

Trans profiles are almost identical, and this is reassuring for several reasons, as detailed in the reliability part later on. The following profiles are those obtained with the GSON setup and are used to develop results obtained with the differential signal profile of the same location (Figure 44). The trans configurations measurements have been performed in July 2017, and the cis configurations measurements have been performed in September 2017.

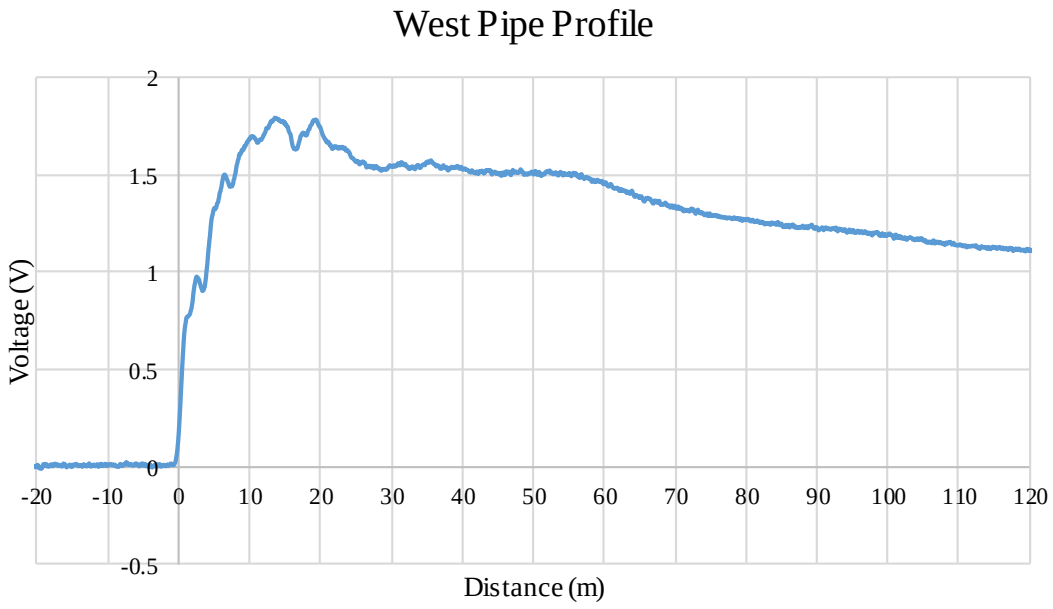

Figure 49: West pipe reflectometry profile (GSON)

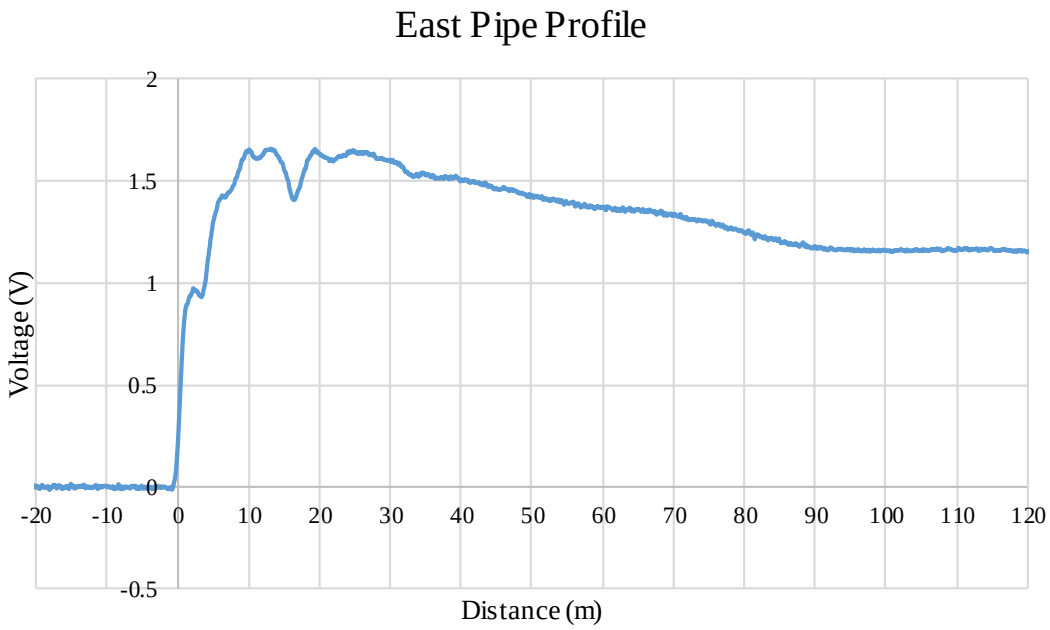

Figure 51: East pipe reflectometry profile (GSON)

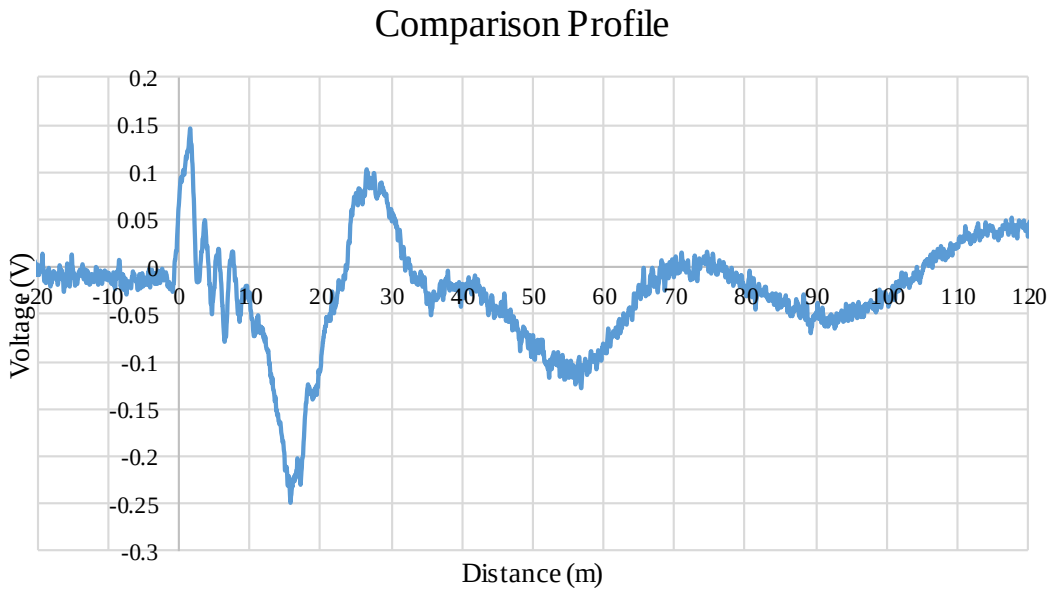

Figure 50: Comparison between east and west pipe profiles

The V shaped pit centered around the 16.5 m distance is of specific interest, as it is the third echo from air/soil interface reflections within the manhole. This distance is indeed exactly 3 times the distance between both ends of the manhole (and therefore also between the oscilloscope probe and generator output patches). Therefore, the corresponding part on the comparison profile cannot be attributed to coating defects. However, defects on the west pipe can be recognized at 19 m and 55 m, and on the east pipe at 28 and 70 m. The oscillation around 90 m is likely due to an echo between the two first defects on the west pipe.

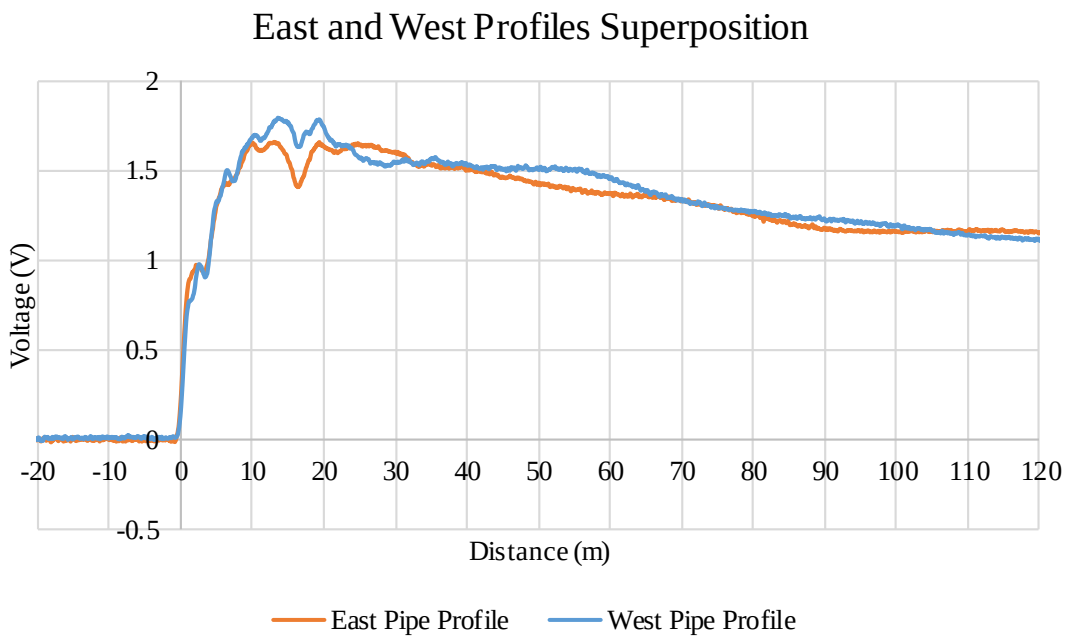

Figure 52: East and west pipe reflectometry profile (GSON)

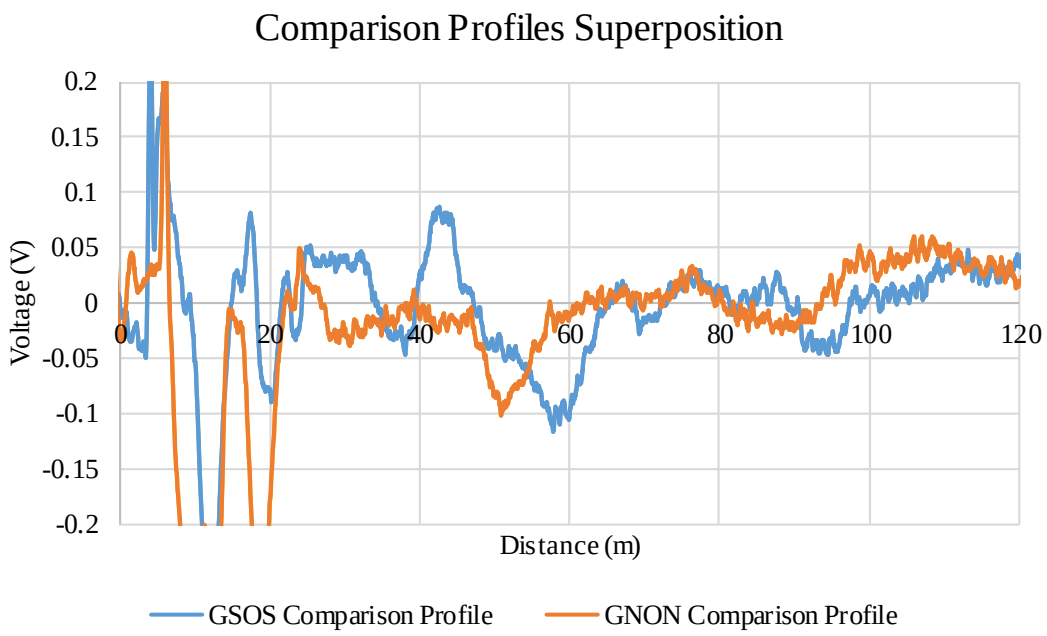

Figure 53: GSOS and GNON comparison profiles superposition

It is important to note the coherence between the grounded signal profiles and the differential signal profiles, as on the differential signal profile reflections will be most important at distances where an electrical path from on pipe to the other pipe, through the defects on their coatings, can occur. The distance of the defects as seen with the GSON and GNON configurations are the same, which is coherent with the paradigm of reflectometry we defined for our works. Furthermore, a characteristic lag can readily be observed between the GSOS and the GNON comparison profiles, which indicates that the defects read are all located on the northern side of the manhole. It is a coincidence that all those defects are on the same side, but on this location it is coherent with what we know of the state of repair of the characterized pipelines.

Reliability considerations

Trans configurations yields very similar profiles (see figures 54 and 55), and that has several consequences. First, it a proof that the indications read are not the product of some elaborate ringing inside the manhole. It also shows that asymmetries built in the system of parallel pipelines as transmission line, such as diffusion chambers, change of pipeline diameters, et cetera within the manhole are acceptable discontinuities that do not jeopardize the reflectometry profile as a whole. Furthermore, it ensues from this similarity that there is no significant velocity difference for the signal between the air or soil medium.

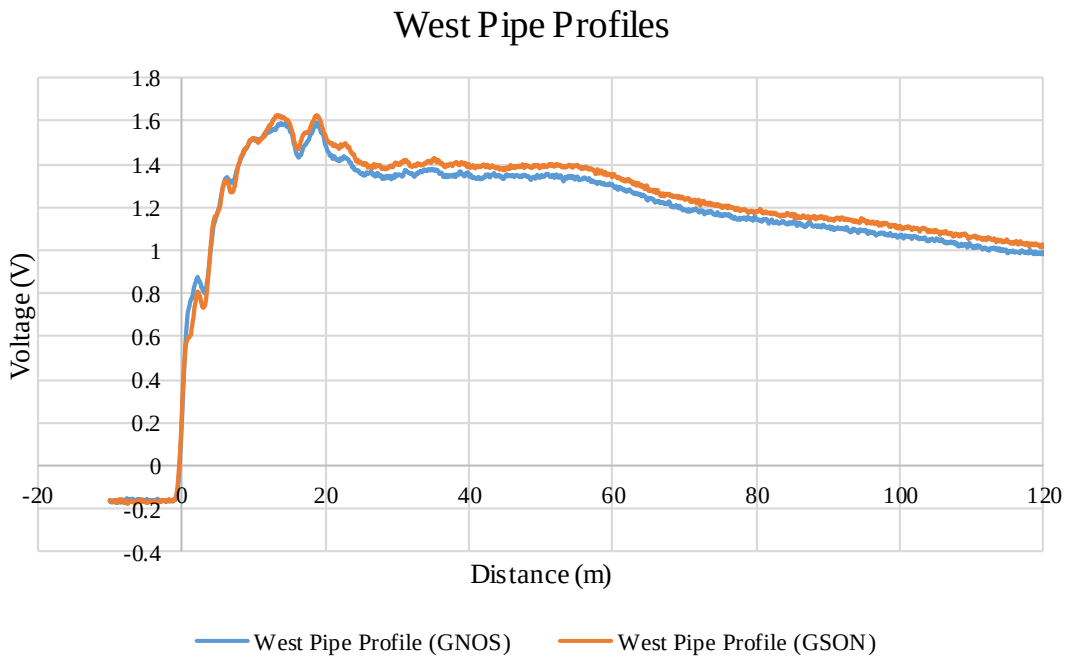

Figure 54: West pipe profiles superposition (GSON and GNOS)

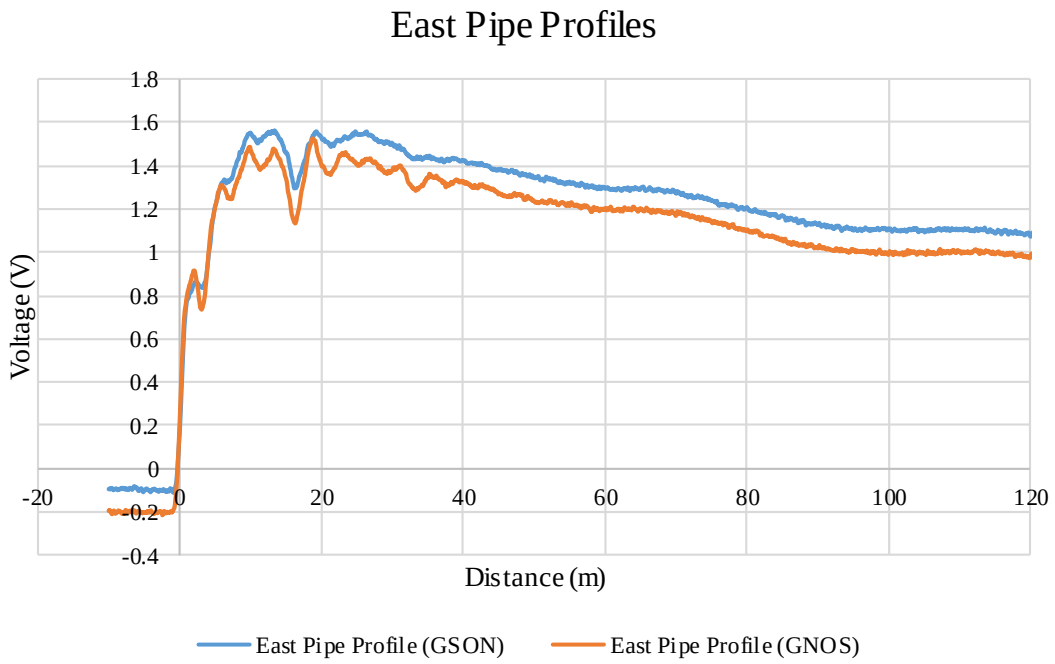

Figure 55: East pipe profiles comparison superposition (GSON and GNOS)

Also fundamental for reliability purposes are the notion of repeatability and reproducibility of results. Both have been ensured during field testing. This in no trivial feature in the harsh environment of densely urbanized cities, on pipelines subjects to multiple induced AC currents, those conditions have proven fatal to other technologies, specifically ACVG/DCVG. Displaying results obtained with measurements performed at different times of the day, figures 56 and 57 show the repeatability of the technique. Displaying results obtained at different times of the year, figure 58 show the reproducibility of the technique.

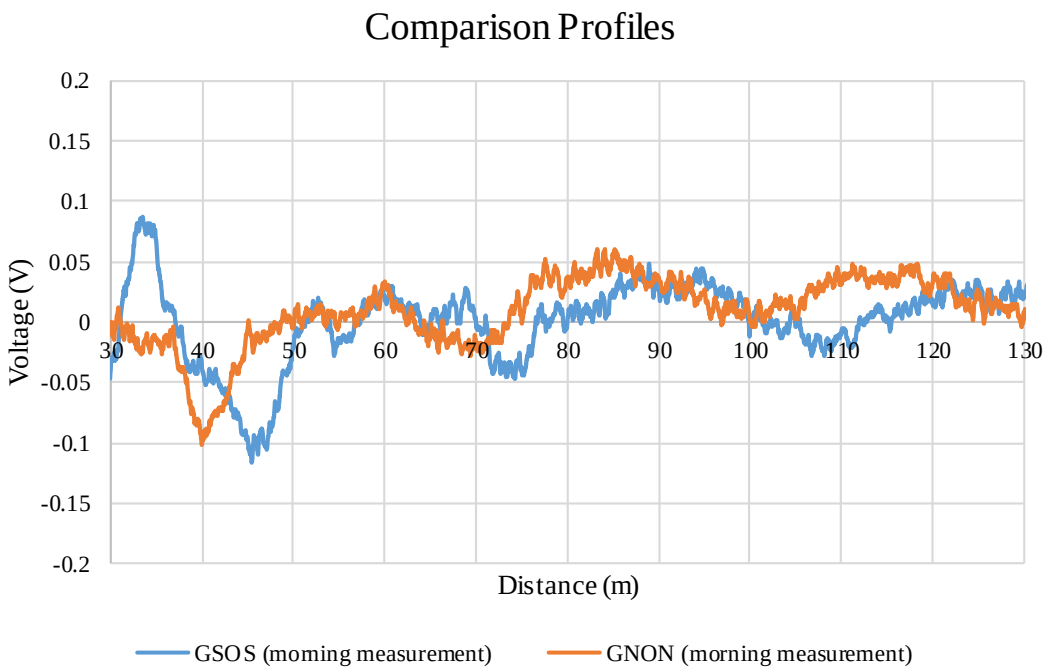

Figure 57: Comparison profiles of morning measurements

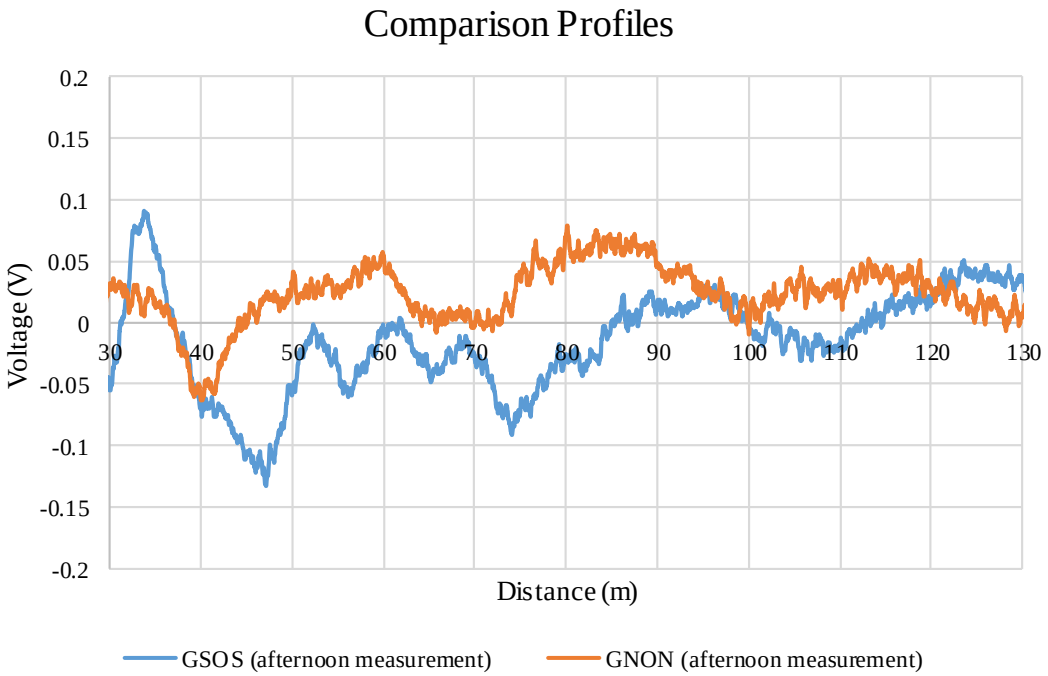

Figure 56: Comparison profiles of afternoon measurements

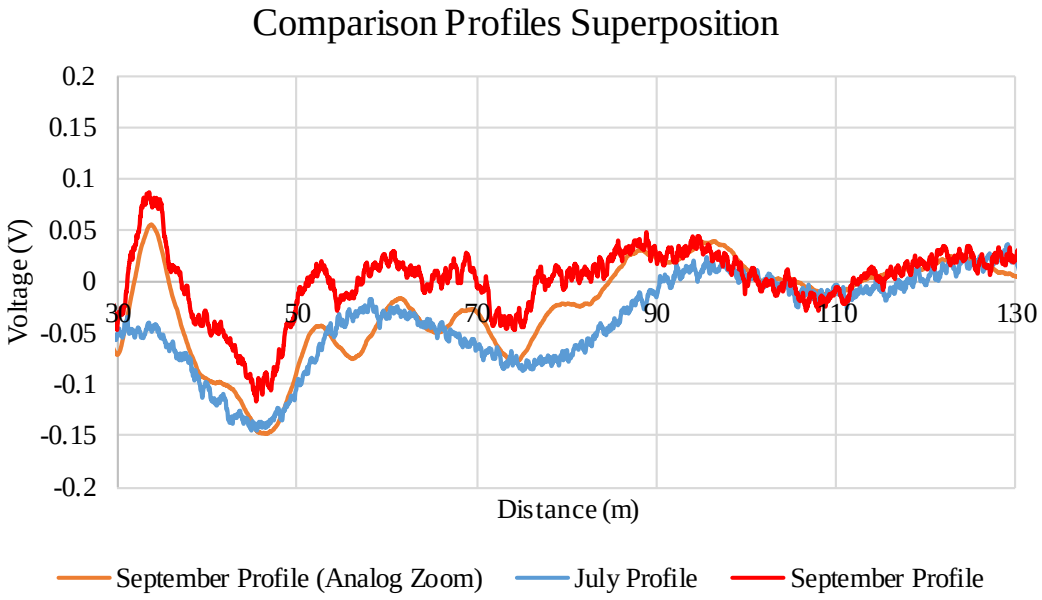

Figure 58: Superposition of comparison profiles performed at different times of the year

Further improvements to this technology will likely include the use of a power amplifier for the waveform generator, in order to increase the sheer strength of the signal. Given the frequencies used (above 50 kHz) this kind of signals is harmless for the assets. Also, performing measurements in manholes is somehow practical for access, but generates unwanted air/soil interface reflections. Having connection points for the oscilloscope probe and the waveform generator without unearthing the pipelines would be ideal.

CHAPTER V

CONCLUSIONS

Inspired by the electrochemical impedance characterization of defect in coal tar coatings on pipes sample in laboratory conditions, research within this thesis has been focused on the detection of current leakage in pipeline systems. In the opinion of the author of this thesis, reflectometry has been found to be the best method to achieve such results in challenging field conditions. To the knowledge of the author, it also happens to never having been tried before or written about in the literature in the way determined by those findings.

The field results have shown efficiency of the method to detect and locate current leakages from the pipes at close locations. Due to the correlation between steepness of the reflection and distance of the event, and due to the possible occurrence of multiple reflection on the two pipes used, sensibility of the methods starts to drop for distances longer than a few thousand feet.

Additional work is required to mature this reflectometry technique into a fully operational technology. The aim of this thesis was to present a convincing case that the paradigm it defines for reflectometry used in pipelines is relevant and well-suited for the detection and location of coating defects, and at least better suited for that latter purpose than classical DVCG techniques in urban environments.

Broader applications are envisioned, such as coaxial systems in refineries, and other parallel structures coated with an insulating coating.

REFERENCES

[1] H.H. Skilling "Electric Transmission Lines", Mc Graw-Hill, 1951

[2] R.W.P. King, "Transmission Line Theory", Mc Graw-Hill, 1955

[3] M.P. Zsigmond, R.H. Johnston, "Simulation of Pipeline Holiday Detection by Time Domain Reflectometry" IEEE Trans. p 961, 1990

[4] H.G. Dwight, "Skin effect in tubular and flat conductors" AIEE Trans. p 1379, 1918

[5] A. Cataldo et al., "Recent advances in the TDR-based leak detection system for pipeline inspection", Measurement p 347, 2017

[6] C.M. Furse, "Reflectometry for Structural Health Monitoring" Lecture Notes in Electrical Engineering, Vol 96, p 159, 2011

[7] J.R. Wait, "Electromagnetic wave propagation along a buried insulated wire" Canadian Journal of Physics, Vol 50, p 2402, 1972

[8] M.C. Miller Co., Inc, "DC Voltage Gradient (DCVG) Surveys Using MCM's Integrated Pipeline Survey Test Equipment and Database Management Package", DCVG Training Manual, 1998

[9] NACE "Control of External Corrosion on Underground or Submerged Metallic Piping System" SP0169-2007